Dissertation

Study of a constrained hyperbolic free boundary problem involving fluid motion based on variational approach and particle method

Graduate School of
Natural Science and Technology
Kanazawa University

Major subject:
Division of Mathematical
and Physical Sciences

Course:
Computational Science

School registration No.: 1023102011
Name: Nguyen Tri Cong
Chief advisor: Seiro OMATA

Abstract

In this research, we study hyperbolic problem with volume preservation, where a free boundary appears. This problem can be obtained by examining the motion of a droplet on plane. In this phenomenon, the drop is divided into two interacting parts: a film representing the surface of the drop, and the fluid inside the film. The motion of the liquid is described by equation of fluid dynamics (Euler equations). The film, which determines a (moving) boundary for the liquid inside, is considered to be the graph of a scalar function. Free boundary, volume constraint and contact angle are three main features of the model of the film. The underlying surface, on which the droplet rests, plays the role of an obstacle to the motion and gives rise to free boundary. Moreover, the volume preservation constraint is obtained from assumption that the volume of the drop does not change. Finally, there is a positive contact angle on the boundary of the region where the drop touches the surface. The hyperbolic free boundary problem with volume conservation constraint is solved by discrete Morse flow method. Moreover, a model taking into account both the surface and the liquid body is solved by combining discrete Morse flow and smoothed particle hydrodynamics method.

Contents

List of Figures

Chapter 1

Introduction

In this study, we develop a simple model for the motion of a droplet on a plane, especially on an inclined plane. The hyperbolic free-boundary problem under the volume conservation constraint plays an important role in this model. The droplet consists of two parts: a film and liquid filling inside the film. The film must have constant volume, i.e, the volume of the region between the film and the underlying surface has to be constant in time. Because of this point, we shall see that a complicated non-local term appears in the model equation. Furthermore, the positive contact angle is the main feature of the drop on plane. In the equilibrium case, the contact angle θ of the droplet depends on the properties of the liquid and the material on which the droplet is lying [19]. It is described by Young's equation

$$\gamma_{SG} - \gamma_{SL} = \gamma_{LG} \cos\theta, \tag{1.1}$$

where γ_{SG} is the solid surface tension, γ_{LG} is the liquid surface tension, and γ_{SL} is the solid/liquid interfacial surface tension (Figure 1.1).

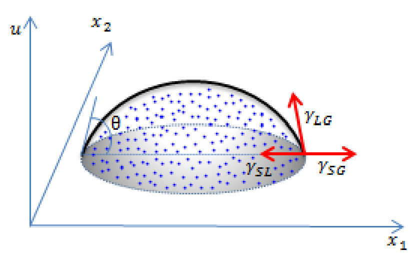

Figure 1.1: The equilibrium of droplet on plane.

In our work, $\theta < 90^0$ is consistently considered. Therefore, the shape of film can be described as a scalar function

$$u : (0,T) \times \Omega \longrightarrow \boldsymbol{r},$$

where $(0,T)$ is the time interval and Ω is the domain where the motion is considered. The set where the film touches the plane is referred as the free boundary. The resulting problem for the membrane is a free boundary equation with a complicated nonlocal term. We shall obtain governing equation in Chapter 2. It has the following form

$$\chi_{u>0}\sigma u_{tt} = \gamma_g \Delta u - \rho g u \chi_{u>0} - R^2 \chi'_{\varepsilon}(u) + \lambda. \tag{1.2}$$

This equation with initial conditions and boundary condition can be solved by the variational method, namely discrete Morse flow, which is explained in details in Chapter 3.

For fluid inside the film, we consider the fluid flow following the Euler equations

$$\begin{aligned} \frac{D\rho}{Dt} + \rho \nabla . \boldsymbol{v} &= 0, \text{ in } \cup_{t\in(0,T)} \Omega_f(t) \times \{t\}, \\ \frac{D\boldsymbol{v}}{Dt} &= -\frac{1}{\rho}\nabla P + \boldsymbol{g}, \text{ in } \cup_{t\in(0,T)} \Omega_f(t) \times \{t\}, \end{aligned}$$

where $\boldsymbol{v}$ is the velocity, P is the pressure and $\boldsymbol{g}$ is the gravitation force. These equations are solved by smooth particle hydrodynamic method. The liquid and the membrane interact in the model via pressure forces, therefore the outer force term plays an important roles in this case.

To continue this Chapter, Chapter 2 will present the model equation for the surface of the droplet, introducing the discrete Morse flow method which is described in details on the example of the hyperbolic equation in the Chapter 3. Chapter 4 represents the basic of smooth particle hydrodynamic method which uses to solve Euler equations. In Chapter 5, the discrete Morse flow is use to construct an approximation solution of the hyperbolic equation. Chapter 6 introduces the couple model which combines the above mentioned hyperbolic equation for film and Euler equations for the fluid filling the film. Chapter 7 draws important conclusions of the research and suggestions some recommendations for further studies.

Notations

We provide a list of notations used in the thesis

$\mathbf{N}$	natural numbers,
$\mathbf{R}^m$	m dimensional real Euclidean space ($\mathbf{R} = \mathbf{R}^1$),
Ω	bounded domain in $\mathbf{R}^m$ with Lipschitz boundary, corresponding to the spatial region, where the equation is solved,
$\partial\Omega$	boundary of domain Ω,
$\|\Omega\|$	the Lebesgue measure of Ω,
$\overline{\Omega}$	closure of the set Ω,
T	a positive real value representing the final time,
Q_T	the open time-space cylinder $(0,T) \times \Omega$,
V	a positive real value representing the volume,
κ, κ_V	sets of functions from certain spaces satisfying the volume constraint,
u	unknown function,
u_t	partial derivative u respect to time t $(= \frac{\partial u}{\partial t})$,
∇u	gradient of u with respect to spatial variables $(= (u_{x1}, u_{x2}, \ldots, u_{xm}))$,
$\triangle u$	the Laplace operator respect to space $(= \frac{\partial^2 u}{\partial x_1^2} + \frac{\partial^2 u}{\partial x_2^2} + \ldots + \frac{\partial^2 u}{\partial x_m^2})$,
$u\|_{\partial\Omega}$	the trace of u on $\partial\Omega$,
u_0, v_0	initial data (shape and velocity, respectively),
λ	Lagrange multiplier, nonlocal term originating in the volume constraint,
h	positive real value, time step of the discretization in time,
a.e.	means "almost everywhere" or "almost every",
$\{u > 0\}$	set of point (t,x) from Q_T, for which $u(t,x) > 0$,
$\chi_{u>0}$	characteristic (or indicator) function of the set $\{u > 0\}$,
C	denotes a generic positive constant, independent of parameters in equation,
Ω_f	the domain filled with fluid,
$\boldsymbol{v}$	the velocity of fluid,
$\boldsymbol{r}$	the position of fluid,
$\boldsymbol{n}$	the unit outer normal vector of the membrane,
$\boldsymbol{g}$	the gravitation force,
P	the pressure of fluid,
ρ	the density of fluid,

σ	the area density of membrane,
m	the mass of fluid,
$\frac{D}{Dt}$	material derivative $\left(=\frac{\partial}{\partial t}+\boldsymbol{v}.\nabla\right)$,
W	the interpolating kernel,
c	the sound speed,
$C(\Omega)$	continuous functions $u:\Omega\longrightarrow\mathbf{R}$
$C^k(\Omega)$	functions $u:\Omega\longrightarrow\mathbf{R}$ that are k-times continuously differentiable,
$C^\infty(\Omega)$	functions $u:\Omega\longrightarrow\mathbf{R}$ that are infinitely differentiable,
$C_0^\infty(\Omega)$	functions $C^\infty(\Omega)$ with compact support
$L^p(\Omega)$	functions $u:\Omega\longrightarrow\mathbf{R}$ that are Lebesgue measurable and $\|u\|_{L^p(\Omega)}<\infty$, where $\|u\|_{L^p(\Omega)}=(\int_\Omega|u|^p dx)^{\frac{1}{p}}$,
$L^\infty(\Omega)$	functions $u:\Omega\longrightarrow\mathbf{R}$ that are Lebesgue measurable and $\|u\|_{L^\infty(\Omega)}<\infty$, where $\|u\|_{L^\infty(\Omega)}=$ess $sup_\Omega|u|$,
$W^{k,p}(\Omega)$	locally summable functions $u:\Omega\longrightarrow\mathbf{R}$ such that for each multiindex α with $\lvert\alpha\rvert\leq k$, $D^\alpha u$ exists in weak sense and belongs to $L^p(\Omega)$. The norm is defined as follows:

$$\|u\|_{W^{k,p}(\Omega)}=\left(\sum_{|\alpha|\leq k}\int_\Omega|D^\alpha u|^p dx\right)^{\frac{1}{p}},$$

$$\|u\|_{W^{k,\infty}(\Omega)}=\sum_{|\alpha|\leq k} ess\ \mathbf{sup}_\Omega|D^\alpha u|,$$

$H^k(\Omega)$	$=W^{k,2}(\Omega)$,
$H_0^1(\Omega)$	the closure of $C_0^\infty(\Omega)$ in $H^1(\Omega)$,
$L^p(0,T;X)$	measurable functions $u:[0,T]\longrightarrow X$ with $\|u\|_{L^p(0,T;X)}<\infty$, where $\|u\|_{L^p(0,T;X)}=(\int_0^T\|u\|_X^p dt)^{\frac{1}{p}}$,
$L^\infty(0,T;X)$	measurable functions $u:[0,T]\longrightarrow X$ with $\|u\|_{L^\infty(0,T;X)}<\infty$, where $\|u\|_{L^\infty(0,T;X)}=ess\ \mathbf{sup}_{0\leq t\leq T}\|u\|_X$,
$W^{1,p}(0,T;X)$	functions $u\in L^p(0,T;X)$ such that u_t exists in the weak sense and belongs to $L^p(0,T;X)$. The norm is

$$\|u\|_{W^{1,p}(0,T;X)}=\left(\int_0^T\|u(t)\|_X^p+\|u_t(t)\|_X^p dt\right)^{\frac{1}{p}},$$

$W^{1,\infty}(0,T;X)$	functions $u \in L^\infty(0,T;X)$ such that u_t exists in the weak sense and belongs to $L^\infty(0,T;X)$. The norm is $$\|u\|_{W^{1,\infty}(0,T;X)} = ess\ \mathbf{sup}_{0\le t\le T}(\|u(t)\|_X + \|u_t(t)\|_X),$$
$H^1(0,T;X)$	$= W^{1,2}(0,T;X)$,
$C_0^\infty(\Omega;\mathbf{R}^m)$	function $u : \Omega \to \mathbf{R}^m$, with $u_i \in C_0^\infty(\Omega), i = 1, 2, .., m$,

Chapter 2

Modelling of the surface of a droplet

Modelling of the motion of a droplet consists of two stages: deriving the model of the film representing the surface of the drop and deriving the model of the fluid inside the film. In this Chapter, we focus on the film model.

2.1 A droplet on the plane

In this case, we consider a droplet on a plane. For simplicity, we assume that the area density of the surface of the drop is constant and that the surface tension is homogeneous. In addition, the contact angle of $\theta < 90°$ is our consistent consideration.

Examining the equilibrium shape of the droplet is our starting point. From the assumption of the contact angle being less than 90^0 the surface of the droplet can be described by the graph of scalar function below

$$u : \Omega \times (0, T) \longrightarrow \mathbf{R},$$

where $(0, T)$ is the time interval and $\Omega \subset \mathbf{R}^m (m \in \mathbf{N} \setminus \{0\})$ is the domain where the motion is considered. The boundary $\partial\Omega$ is assumed to be Lipschitz on which Dirichlet condition is prescribed. The film is assumed not to go under the plane. Moreover, the volume preservation of the film is crucial assumption

$$\int_\Omega u\chi_{u>0} dx = V > 0.$$

The surface energy of the stable droplet can be written as

$$E = \int_\Omega \gamma_g \sqrt{1+|\nabla u|^2}\chi_{u>0}dx + \int_\Omega \gamma_s \chi_{u>0}dx \tag{2.1}$$

where $\gamma_g = \gamma_{LG}, \gamma_s = \gamma_{SL} - \gamma_{SG}$ (Figure. 1.1).

If we assume that the minimizer exists and is smooth, we obtain the following result (see [15]).

Lemma 1. *Let the minimizer of (2.1) be smooth in* $\overline{\{u>0\}}$. *Then Young's equation*

$$\gamma_s = -\gamma_g \cos\theta$$

hold on $\partial\{u>0\}$.

Proof. We denote

$$u_\varepsilon = V\frac{u+\varepsilon\varphi}{V+\varepsilon\Phi}$$

where $\Phi = \int_\Omega \varphi dx$. Then we have

$$\begin{aligned}
0 &= \lim_{\varepsilon\to 0}\frac{1}{\varepsilon}(E(u_\varepsilon)-E(u)) \\
&= \lim_{\varepsilon\to 0}\frac{\gamma_g}{\varepsilon}\int_\Omega \Big(\sqrt{1+\frac{|\nabla u+\varepsilon\nabla\varphi|^2}{(1+\varepsilon\Phi/V)^2}}\chi_{u_\varepsilon>0} - \sqrt{1+|\nabla u|^2}\chi_{u>0}\Big)dx \\
&+ \lim_{\varepsilon\to 0}\frac{1}{\varepsilon}\int_\Omega \gamma_s(\chi_{u_\varepsilon>0}-\chi_{u>0})dx \\
&= \gamma_g\int_\Omega \frac{\nabla u\nabla\varphi - \frac{1}{V}|\nabla u|^2\Phi}{\sqrt{1+|\nabla u|^2}}\chi_{u>0}dx \\
&= \gamma_g\int_\Omega \Big(\frac{\nabla u\nabla\varphi}{\sqrt{1+|\nabla u|^2}} - \frac{1}{V}\frac{|\nabla u|^2}{\sqrt{1+|\nabla u|^2}}\Phi\Big)\chi_{u>0}dx \\
&= \gamma_g\int_\Omega \Big(\frac{\nabla u\nabla\varphi}{\sqrt{1+|\nabla u|^2}} - \lambda\varphi\Big)\chi_{u>0}dx,
\end{aligned}$$

where $\lambda = \frac{1}{V}\int_\Omega \frac{|\nabla u|^2}{\sqrt{1+|\nabla u|^2}}dx$.

Using Green's theorem we have following form

$$\gamma_g\int_\Omega \Big(\nabla.\Big(\frac{\nabla u}{\sqrt{1+|\nabla u|^2}}\Big)+\lambda\Big)\varphi dx = 0, \quad \forall\varphi\in C_0^\infty(\Omega\cap\{u>0\}) \tag{2.2}$$

On the other hand, we can carry out the so-called inner variation of (2.1), which uses the perturbation

$$u_\varepsilon = \frac{V}{V_\varepsilon} u(\tau_\varepsilon^{-1}(x)),$$

where

$$\tau_\varepsilon(x) = x + \varepsilon\eta(x), \quad \eta \in C_0^\infty(\Omega, \mathbf{R}^m)$$

with Jacobian

$$|D\tau_\varepsilon| = 1 + \varepsilon(\nabla.\eta) + o(\varepsilon), \quad \varepsilon \to 0,$$

and V_ε is determined so that the perturbation preserves volume:

$$V_\varepsilon = \int_\Omega u(\tau_\varepsilon^{-1}(x))dx = \int_\Omega u(y)|D\tau_\varepsilon(y)|dy = V + \varepsilon \int_\Omega u(\nabla.\eta)dx + o(\varepsilon), \quad \varepsilon \to 0.$$

Noting that if we denote

$$y_i(x) = x_i + \varepsilon\eta_i(x)$$

then

$$\begin{aligned}
\frac{\partial y_i}{\partial x_j}(x) &= \delta_{ij} + \varepsilon \frac{\partial \eta_i}{\partial x_j}(x) \\
\frac{\partial x_j}{\partial y_i}(y) &= \delta_{ji} - \varepsilon \frac{\partial \eta_j}{\partial x_i}(x) + o(\varepsilon), \quad \varepsilon \to 0. \\
\frac{\partial u_\varepsilon}{\partial y_i}(y) &= \frac{V}{V_\varepsilon} \sum_j \frac{\partial u}{\partial x_j}(x) \frac{\partial x_j}{\partial y_i}(y) \\
&= \frac{V}{V_\varepsilon} \sum_j \frac{\partial u}{\partial x_j}(x) \Big(\delta_{ji} - \frac{\partial \eta_j}{\partial x_i}(x) + o(\varepsilon) \Big), \quad \varepsilon \to 0 \\
&= \frac{V}{V_\varepsilon} \left(\frac{\partial u}{\partial x_i}(x) - \varepsilon \sum_j \frac{\partial u}{\partial x_j} \frac{\partial \eta_j}{\partial x_i}(x) \right) + o(\varepsilon), \quad \varepsilon \to 0. \\
&= \frac{V}{V_\varepsilon} \left(\frac{\partial u}{\partial x_i}(\tau_\varepsilon^{-1}(y)) - \varepsilon \sum_j \frac{\partial u}{\partial x_j} \frac{\partial \eta_j}{\partial x_i}(\tau_\varepsilon^{-1}(y)) \right) + o(\varepsilon), \quad \varepsilon \to 0.
\end{aligned}$$

and employing the substitution $x=\tau_\varepsilon^{-1}(y)$, we have

$$
\begin{aligned}
0 &= \lim_{\varepsilon\to 0}\frac{1}{\varepsilon}(E(u_\varepsilon)-E(u))\\
&= \lim_{\varepsilon\to 0}\frac{\gamma_g}{\varepsilon}\int_\Omega\left(\sqrt{1+\frac{V^2}{V_\varepsilon^2}\sum_i\Big(\frac{\partial u}{\partial x_i}-\varepsilon\sum_j\frac{\partial u}{\partial x_j}\frac{\partial \eta_j}{\partial x_i}\Big)^2}(1+\varepsilon\nabla.\eta)-\sqrt{1+|\nabla u|^2}\right)\chi_{u>0}dx\\
&\quad+\lim_{\varepsilon\to 0}\frac{1}{\varepsilon}\int_\Omega(\gamma_s(\tau_\varepsilon)(1+\varepsilon\nabla.\eta)-\gamma_s)\chi_{u>0}dx\\
&= \lim_{\varepsilon\to 0}\frac{\gamma_g}{\varepsilon}\int_\Omega\frac{2\varepsilon\nabla.\eta+\frac{V^2}{V_\varepsilon^2}\Big(|\nabla u|^2-2\varepsilon\sum_{i,j}\frac{\partial u}{\partial x_i}\frac{\partial u}{\partial x_j}\frac{\partial \eta_j}{\partial x_i}\Big)(1+2\varepsilon\nabla.\eta)-|\nabla u|^2}{2\sqrt{1+|\nabla u|^2}}\chi_{u>0}dx\\
&\quad+\int_\Omega\left(\frac{\gamma_s(\tau_\varepsilon)-\gamma_s}{\varepsilon}+\gamma_s(\tau_\varepsilon)(\nabla.\eta)\right)\chi_{u>0}dx\\
&= \gamma_g\int_{\{u>0\}}\left(\frac{(1+|\nabla u|^2)(\nabla.\eta)-\nabla u^T D\eta\nabla u}{\sqrt{(1+|\nabla u|^2}}-\lambda u(\nabla.\eta)\right)dx+\int_{\{u>0\}}\nabla.(\gamma_s\eta)dx.
\end{aligned}
$$

Using Green's theorem, we have

$$
\begin{aligned}
\int_{\{u>0\}}u(\nabla.\eta)dx &= -\int_{\{u>0\}}\nabla u.\eta dx+\int_{\partial\{u>0\}}u(\eta.\nu)dS\\
\int_{\{u>0\}}\nabla.(\gamma_s\eta)dx &= -0+\int_{\partial\{u>0\}}\gamma_s(\eta.\nu)dx\\
\int_{\{u>0\}}\frac{(1+|\nabla u|^2)(\nabla.\eta)}{\sqrt{(1+|\nabla u|^2}}dx &= -\int_{\{u>0\}}\frac{\nabla u^T D^2u\eta}{\sqrt{1+|\nabla u|^2}}dx+\int_{\partial\{u>0\}}\sqrt{1+|\nabla u|^2}(\eta.\nu)dS\\
\int_{\{u>0\}}\frac{\nabla u}{\sqrt{(1+|\nabla u|^2}}.\nabla(\nabla u.\eta)dx &= -\int_{\{u>0\}}\nabla.\left(\frac{\nabla u}{\sqrt{1+|\nabla u|^2}}\right)(\nabla u.\eta)dx\\
&\quad+\int_{\partial\{u>0\}}(\nabla u.\eta)\left(\frac{\nabla u.\nu}{\sqrt{1+|\nabla u|^2}}\right)dS
\end{aligned}
$$

On the other hand, we have

$$
\int_{\{u>0\}}\frac{\nabla u}{\sqrt{1+|\nabla u|^2}}.\nabla(\nabla u.\eta)dx=\int_{\{u>0\}}\frac{\nabla u^T D^2u\eta+\nabla u^T D\eta\nabla u}{\sqrt{1+|\nabla u|^2}}dx
$$

So we obtain

$$\int_{\{u>0\}} \frac{\nabla u^T D\eta \nabla u}{\sqrt{1+|\nabla u|^2}} dx = -\int_{\{u>0\}} \frac{\nabla u^T D^2 u \eta}{\sqrt{1+|\nabla u|^2}} dx - \int_{\{u>0\}} \nabla . \left(\frac{\nabla u}{\sqrt{1+|\nabla u|^2}} \right) (\nabla u . \eta) dx$$
$$+ \int_{\partial\{u>0\}} (\nabla u . \eta) \left(\frac{\nabla u . \nu}{\sqrt{1+|\nabla u|^2}} \right) dS$$

where $\nu = -\frac{\nabla u}{|\nabla u|}$ is the unit outer normal to $\partial\{u>0\}$.
From these results, we get

$$\begin{aligned} 0 = &\gamma_g \int_{\{u>0\}} \left[\nabla . \left(\frac{\nabla u}{\sqrt{1+|\nabla u|^2}} \right) + \lambda \right] (\nabla u . \eta) dx \\ &+ \int_{\partial\{u>0\}} \left(\gamma_g \left(\sqrt{1+|\nabla u|^2} - \frac{|\nabla u|^2}{\sqrt{1+|\nabla u|^2}} \right) + \gamma_s \right) (\eta . \nu) dS, \end{aligned}$$

Using the result (2.2), which yields:

$$0 = \int_{\partial\{u>0\}} \left(\gamma_g \left(\sqrt{1+|\nabla u|^2} - \frac{|\nabla u|^2}{\sqrt{1+|\nabla u|^2}} \right) + \gamma_s \right) (\eta . \nu) dS, \quad \forall \eta \in C_0^\infty(\Omega, \mathbf{R}^m).$$

We conclude that

$$\gamma_s = -\frac{1}{\sqrt{1+|\nabla u|^2}} \gamma_g \quad \text{on } \partial\{u>0\},$$

On the other the hand, we have $\tan\theta = |\nabla u|$, which yields

$$\gamma_s = -\gamma_g \cos\theta \quad \text{on } \partial\{u>0\}$$

□

We rewrite equation (2.1) as follows:

$$E = \int_\Omega \gamma_g \sqrt{1+|\nabla u|^2} dx + \int_\Omega (\gamma_g + \gamma_s) \chi_{u>0} dx - \gamma_g |\Omega|. \tag{2.3}$$

Now suppose that the gradient of u remains small (i.e, the deformation of the film is very small) then by Taylor expansion we have

$$\sqrt{1+|\nabla u|^2} \simeq 1 + \frac{1}{2} |\nabla u|^2$$

Thus, we can write the approximation of the surface energy (2.3) in the form

$$\tilde{E} = \int_\Omega \frac{\gamma_g}{2}|\nabla u|^2 dx + \int_\Omega R^2 \chi_{u>0} dx \tag{2.4}$$

where $R^2 = \gamma_g + \gamma_s$. Potential energy of fluid surrounded by the film is

$$\rho g \int_\Omega \frac{1}{2} u^2 \chi_{u>0} dx,$$

where ρ is the fluid density. On other hand, the kinetic energy of the vertical movement of the film is given by

$$\int_\Omega \Big(\frac{\sigma}{2} u_t^2 \chi_{u>0}\Big) dx,$$

where σ is the area density of the surface. Therefore, the Lagrangian for the film can be written as

$$L(u,t) = \int_\Omega \Big(\frac{\sigma}{2} u_t^2 \chi_{u>0} - \frac{\gamma_g}{2}|\nabla u|^2 - R^2 \chi_\varepsilon(u) - \frac{1}{2}\rho g u^2 \chi_{u>0}\Big) dx,$$

where $\chi_{u>0}$ in equation (2.4) is replaced by a smoothing function $\chi_\varepsilon \in C^2(\mathbf{R})$ satisfying

$$\chi_\varepsilon(s) = \begin{cases} 1, & \text{if } s \geq \varepsilon, \\ 0, & \text{if } s \leq 0 \end{cases}$$

and $|\chi_\varepsilon'(s)| \leq C/\varepsilon$ for $s \in (0, \varepsilon)$. The purpose of smoothing is to avoid the presence of delta function in the equation [15].

The equation of motion within time interval $(0, T)$ can be defined by

$$J(u) = \int_0^T L(u,t) dt,$$

and the problem is determining the stationary point of functional J in the suitable function space satisfying the given volume constraint $V > 0$.

Problem 1. *Find the stationary state u of functional*

$$J(u) = \int_0^T \int_\Omega \Big(\frac{\sigma}{2} u_t^2 \chi_{u>0} - \frac{\gamma_g}{2}|\nabla u|^2 - R^2 \chi_\varepsilon(u) - \frac{1}{2}\rho g u^2 \chi_{u>0}\Big) dx dt,$$

in the function space

$$K = \left\{ u \in H^1(\Omega_T); u|_{\partial\Omega} = 0, \int_\Omega u\chi_{u>0} = V \right\},$$

where $u_0(x)$ is the initial shape and v_0 is the initial velocity of the film.

Let u be a stationary point of J. We select an arbitrary function $\varphi \in C_0^\infty((0,T) \times (\Omega \cap \{u > 0\}))$, and denote

$$\Phi(t) = \int_\Omega \varphi(t,x)dx.$$

$$u_\varepsilon = (u + \varepsilon\varphi)\frac{V}{V + \varepsilon\Phi}.$$

If A is denoted by $A = \frac{V}{V+\varepsilon\Phi}$ then we obtain

$$\begin{aligned}
&\lim_{\varepsilon\to 0} A = 1,\\
&\lim_{\varepsilon\to 0} A_t = \lim_{\varepsilon\to 0} \frac{\varepsilon V \Phi_t}{(V - \varepsilon\Phi)^2} = 0,\\
&\lim_{\varepsilon\to 0} \frac{dA}{d\varepsilon} = \lim_{\varepsilon\to 0} \frac{V\Phi}{(V - \varepsilon\Phi)^2} = -\frac{\Phi}{V},\\
&\lim_{\varepsilon\to 0} \frac{d}{d\varepsilon} A_t = -\frac{\Phi_t}{V},\\
&\lim_{\varepsilon\to 0} \frac{d}{d\varepsilon} A^2 = -\frac{2\Phi}{V},\\
&\lim_{\varepsilon\to 0} \frac{d}{d\varepsilon} (AA_t) = -\frac{\Phi_t}{V},\\
&\lim_{\varepsilon\to 0} \frac{d}{d\varepsilon} A_t^2 = 0.
\end{aligned} \tag{2.5}$$

Thanks to above relations we can calculate the first derivative of each term in functional $J(u)$:

$$\begin{aligned}
\lim_{\varepsilon\to 0}\frac{d}{d\varepsilon}\int_0^T\int_\Omega \frac{\sigma}{2}[(u_\varepsilon)_t]^2\chi_{u>0}dxdt &= \int_0^T\int_\Omega \sigma\Big[u_t\varphi_t-\frac{1}{V}u_t(u_t\Phi+u\Phi_t)\Big]\chi_{u>0}dxdt\\
&= \int_0^T\int_\Omega \sigma\Big[-u_{tt}\varphi-\frac{1}{V}u_t(u\Phi)_t\Big]\chi_{u>0}dxdt\\
&= \int_0^T\int_\Omega \sigma\Big[-u_{tt}\varphi+\frac{1}{V}u_{tt}u\Phi\Big]\chi_{u>0}dxdt,\\
\lim_{\varepsilon\to 0}\frac{d}{d\varepsilon}\int_0^T\int_\Omega \frac{\gamma_g}{2}|\nabla u_\varepsilon|^2dxdt &= \int_0^T\int_\Omega \gamma_g\Big(\nabla u\nabla\varphi-\frac{1}{V}(\nabla u)^2\Phi\Big)dxdt\\
&= \int_0^T\int_\Omega \gamma_g\Big(-\Delta u\varphi-\frac{1}{V}(\nabla u)^2\Phi\Big)dxdt,\\
\lim_{\varepsilon\to 0}\frac{d}{d\varepsilon}\int_0^T\int_\Omega R^2\chi_\varepsilon(u_\varepsilon)dxdt &= \int_0^T\int_\Omega R^2\chi_\varepsilon'(u)\big(\varphi-\frac{1}{V}u\Phi\big)dxdt,\\
\lim_{\varepsilon\to 0}\frac{d}{d\varepsilon}\int_0^T\int_\Omega \frac{1}{2}\rho g u_\varepsilon^2\chi_{u>0}dxdt &= \int_0^T\int_\Omega \rho g\big(u\varphi-\frac{1}{V}u^2\Phi\big)\chi_{u>0}dxdt
\end{aligned}$$

Since u is a stationary point, we have

$$\begin{aligned}
0 &= \frac{dJ(u_\varepsilon)}{d\varepsilon}\Big|_{\varepsilon=0}\\
&= \int_0^T\int_\Omega\Big(-\sigma u_{tt}\chi_{u>0}+\gamma_g\Delta u-R^2\chi_\varepsilon'(u)-\rho g u\chi_{u>0}\Big)\varphi dxdt\\
&+\frac{1}{V}\int_0^T\int_\Omega\Big(\sigma u u_{tt}\chi_{u>0}+\gamma_g(\nabla u)^2+R^2u\chi_\varepsilon'(u)+\rho g u^2\chi_{u>0}\Big)\Phi dxdt\\
&= \int_0^T\int_\Omega\Big(-\sigma u_{tt}\chi_{u>0}+\gamma_g\Delta u-R^2\chi_\varepsilon'(u)-\rho g u\chi_{u>0}+\lambda\Big)\varphi dxdt
\end{aligned}$$

where

$$\lambda=\frac{1}{V}\int_\Omega\Big(\sigma u u_{tt}\chi_{u>0}+\gamma_g(\nabla u)^2+R^2u\chi_\varepsilon'(u)+\rho g u^2\chi_{u>0}\Big)dx.$$

The strong version of the above formulation is as follows:

$$\chi_{u>0}\sigma u_{tt}=\gamma_g\Delta u-\rho g u\chi_{u>0}-R^2\chi_\varepsilon'(u)+\lambda. \tag{2.6}$$

2.2 A droplet on inclined plane

In the case of a droplet on inclined plane with angle α above equation becomes

$$\chi_{u>0}\sigma u_{tt} = \gamma_g \Delta u - f\chi_{u>0} - R^2\chi'_\varepsilon(u) + \lambda, \tag{2.7}$$

where $f = \rho g(u\cos\alpha - x_1 \sin\alpha)$, here x_1 is the horizontal axis, and

$$\lambda = \frac{1}{V}\int_\Omega \left(\gamma_g|\nabla u|^2 + fu\chi_{u>0} + R^2 u\chi'_\varepsilon(u) + \sigma u_{tt}u\chi_{u>0}\right)dx.$$

Chapter 3

Discrete Morse Flow Method

This Chapter explains *Discrete Morse Flow* (DMF), the variational method used in this study to solve the problem that dependent on time with differential operators for space variables in divergence form. This method was first introduced by N. Kikuchi to solve parabolic problems [1], and also used to solve hyperbolic problems [2], [5]. One of the extensions of this method was used to solve free-boundary problems [3], [4]. Solving volume-preserving problems is the other extension of this method [6], [16]. Particularly, this method can be naturally applied to the free boundary problem with volume constraint in [14], [17].
In this case, we describe the details on the example of the hyperbolic equation. The content in this part is based on [15].

3.1 Mathematical formulation

We consider a bounded domain $\Omega \subset \mathbf{R}^n$ with smooth boundary $\partial\Omega$, on which homogeneous Dirichlet boundary condition is given. Then, with a fixed initial position value $u_0 \in, H_0^1(\Omega)$, and initial velocity $v_0 \in, H_0^1(\Omega)$, we consider the problem:

$$\begin{aligned} u_{tt}(t,x) &= \Delta u(t,x), \quad (t,x) \in \Omega_T = (0,T) \times \Omega, && (3.1) \\ u(t,x) &= 0, \quad (t,x) \in (0,T) \times \partial\Omega, && (3.2) \\ u(0,x) &= u_0(x), \quad x \in \Omega, && (3.3) \\ u_t(0,x) &= v_0(x), \quad x \in \Omega. && (3.4) \end{aligned}$$

First, we fix a large number $N > 0$, determine the time step $h = T/N$. From the initial conditions, we define u_{-1} using a backwards difference $u_{-1} = u_0 - v_0 h$. We then define $u_n \in H_0^1(\Omega)$ for $n = 1, 2, .., N$, to minimize the functional

$$J_n(u) := \int_\Omega \frac{|u - 2u_{n-1} + u_{n-2}|^2}{2h^2} dx + \frac{1}{2}\int_\Omega |\nabla u|^2 dx \tag{3.5}$$

In this functional, we see that the first term is continuous in $L^2(\Omega)$ and the second term is lower-semicontinuous with respect to sequentially weak convergence in $H^1(\Omega)$. The existence of minimizers then follows immediately since the functional are bounded below for each $n = 1, 2, .., N$.

Next step, having obtained the existence of minimizers, we define their piecewise linear time interpolant by

$$u^h(t, x) = \frac{t - (n-1)h}{h} u_n(x) + \frac{nh - t}{h} u_{n-1}(x) \tag{3.6}$$

and a piecewise constant step function by

$$\overline{u}^h(t, x) = u_n(x) \tag{3.7}$$

for $(t, x) \in ((n-1)h, nh] \times \Omega, n = 0, 1, .., N$.

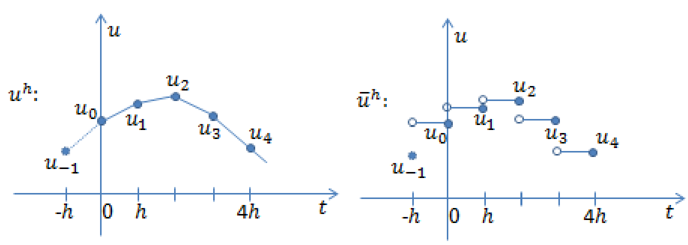

Figure 3.1: Interpolation of minimizers

Because u_n is a minimizer of J_n, the first variation of J_n at u_n vanishes.

Therefore, for any $\varphi \in H_0^1(\Omega)$ we have

$$\begin{aligned}
0 &= \frac{d}{d\varepsilon} J_n(u_n+\varepsilon\varphi)|_{\varepsilon=0} = \lim_{\varepsilon\longrightarrow 0} \frac{J_n(u_n+\varepsilon\varphi)-J_n(u_n)}{\varepsilon} \\
&= \lim_{\varepsilon\longrightarrow 0} \frac{1}{\varepsilon}\int_\Omega \frac{|u_n+\varepsilon\varphi-2u_{n-1}+u_{n-2}|^2-|u_n-2u_{n-1}+u_{n-2}|^2}{2h^2}dx \\
&+ \lim_{\varepsilon\longrightarrow 0} \frac{1}{2\varepsilon}\int_\Omega (|\nabla u_n+\varepsilon\nabla\varphi|^2-|\nabla u_n|^2)dx \\
&= \lim_{\varepsilon\longrightarrow 0}\int_\Omega \frac{(2u_n+\varepsilon\varphi-4u_{n-1}+2u_{n-2})\varphi}{2h^2} + \lim_{\varepsilon\longrightarrow 0}\frac{1}{2}\int_\Omega (2\nabla u_n\nabla\varphi+\varepsilon|\nabla\varphi|^2)dx \\
&= \int_\Omega \frac{u_n-2u_{n-1}+u_{n-2}}{h^2}\varphi dx + \int_\Omega \nabla u_n\nabla\varphi dx \qquad (3.8)
\end{aligned}$$

As we defined for u^h and $\overline{u}^h$ in equation (3.7) and (3.6) we obtain:

$$\int_\Omega \Big[\frac{u_t^h(t)-u_t^h(t-h)}{h}\varphi+\nabla\overline{u}^h\nabla\varphi\Big]dx = 0 \quad \text{for a.e. } t\in(h,T) \ \ \forall\varphi\in H_0^1(\Omega). \tag{3.9}$$

This relation satisfies with any $\tilde{\varphi} \in C([0,T])$. Thus, we have:

$$\int_h^T\int_\Omega \Big[\frac{u_t^h(t)-u_t^h(t-h)}{h}\varphi+\nabla\overline{u}^h\nabla\varphi\Big]dxdt = 0 \ \ \forall\varphi\in L^2(0,T;H_0^1(\Omega)). \tag{3.10}$$

Now, we want to take limit of time step h to zero. However, we need some more estimate. We state it in the following Lemma.

Lemma 2. *Suppose Ω is a bounded domain with smooth boundary. Let $J_n, n = 2,3,..,N$, be the functionals defined by (3.5) and let u_n be corresponding minimizers in $H_0^1(\Omega)$. Define functions $\overline{u}^h$ and u^h by (3.7),(3.6) and assume $h \le 1$. Then the following estimate holds*

$$\|u_t^h(t)\|^2_{L^2(\Omega)} + \|\nabla\overline{u}_t^h(t)\|^2_{L^2(\Omega)} \le C_E \textit{ for a.e. } t\in(0,T) \tag{3.11}$$

where constant C_E is defined in the proof and is independent of h.

Proof. We replace φ in (3.8)by $\varphi := u_n - u_{n-1}$. This yields

$$\int_\Omega \frac{u_n-2u_{n-1}+u_{n-2}}{h^2}(u_n-u_{n-1})dx + \int_\Omega (\nabla u_n-\nabla u_{n-1})\nabla u_n dx = 0.$$

Using the inequality

$$\frac{a^2}{2} - \frac{b^2}{2} \leq (a-b)a, \forall a, b \in \mathbb{R}$$

for two term of this, we get

$$\int_\Omega \Big[(\frac{u_n - u_{n-1}}{h})^2 - (\frac{u_{n-1} - u_{n-2}}{h})^2 + |\nabla u_n|^2 - |\nabla u_{n-1}|^2 \Big] dx \leq 0$$

$$\int_\Omega \Big[(\frac{u_n - u_{n-1}}{h})^2 + |\nabla u_n|^2 \Big] dx \leq \int_\Omega \Big[(\frac{u_{n-1} - u_{n-2}}{h})^2 + |\nabla u_{n-1}|^2 \Big] dx.$$

Since these inequalities are summed from $n = 1$ to $k \leq N$. Thus, we obtain

$$\begin{aligned} \int_\Omega \Big[(\frac{u_k - u_{k-1}}{h})^2 + |\nabla u_k|^2 \Big] dx &\leq \int_\Omega \Big[(\frac{u_0 - u_{-1}}{h})^2 + |\nabla u_0|^2 \Big] dx \\ &= \int_\Omega \Big[(v_0)^2 + |\nabla u_0|^2 \Big] dx \\ &= \|v_0\|^2_{L^2(\Omega)} + \|\nabla u_0\|^2_{L^2(\Omega)}. \end{aligned}$$

We know $u_t^h(t) = \frac{u_k - u_{k-1}}{h}$ and $\nabla u_k = \nabla \overline{u}_t^h$ for $t \in ((k-1)h, kh), k = 0, 1, .., N$, then we get the estimate (3.11). □

Thanks to the estimate(3.11), we can apply the theorem by Eberlein and Shmulyan to extract a subsequence $\{\nabla \overline{u}^{h_k}\}_{k \in \mathbb{N}}$ which converges weakly in $L^2(Q_T)$ to the function $\mathbf{v}$. From the sequence $\{h_{k_l}\}_{l \in \mathbb{N}}$ so that $\{u_t^{h_{k_l}}\}_{l \in \mathbb{N}}$ converges weakly in $L^2(Q_T)$ to a function U. In the sequence, we often use this logic but we shall omit this lengthy explanation and subscripts, and simply write

$$\nabla \overline{u}_t^h \rightharpoonup \mathbf{v} \quad \text{in } (L^2(Q_T))^m, \tag{3.12}$$

$$u_t^h \rightharpoonup U \quad \text{in } L^2(Q_T). \tag{3.13}$$

We should now show that there is a function $u \in L^2(0, T; H_0^1(\Omega))$ such that $\mathbf{v} = \nabla u$ and $U = u_t$ in $L^2(Q_T)$. To this end, a more detailed analysis is needed. First, we estimate the norm of the difference of the approximate functions $\overline{u}^h$ and u^h. Let $t \in ((n-1)h, nh)$. Then

$$\begin{aligned}
\|\overline{u}^h(t) - u^h(t)\|^2_{L^2(\Omega)} &= \int_\Omega (\overline{u}^h - u^h)^2 dx \\
&= \int_\Omega \big(u_n - \frac{t-(n-1)h}{h} u_n - \frac{nh-t}{h} u_{n-1}\big)^2 dx \\
&= \int_\Omega \big(\frac{nh-t}{h}\big)^2 (u_n - u_{n-1})^2 dx \\
&\leq \int_\Omega (u_n - u_{n-1})^2 dx = h^2 \int_\Omega (u_t^h)^2 dx \\
&\leq C_E^2 h^2.
\end{aligned}$$

This means that

$$\|\overline{u}^h - u^h\|_{L^2(\Omega)} \leq Ch \text{ for a.e. } t \in (0,T).$$

We have further

$$\begin{aligned}
\|u^h\|^2_{L^2(Q_T)} - \|\overline{u}^h\|^2_{L^2(Q_T)} &= \int_0^T \int_\Omega (((u^h)^2 - \overline{u}^h)^2) dx dt \\
&= \sum_{n=1}^N \int_{(n-1)h}^{nh} \int_\Omega \Big[\big(\frac{t-(n-1)h}{h} u_n - \frac{nh-t}{h} u_{n-1}\big)^2 - u_n^2\Big] dx dt \\
&= \sum_{n=1}^N \int_\Omega \big(-\frac{2h}{3} u_n^2 + \frac{h}{3} u_n u_{n-1} + \frac{h}{3} u_{n-1}^2\big) dx \\
&\leq \frac{h}{6} \sum_{n=1}^N \int_\Omega (-4u_n^2 + u_n^2 + u_{n-1}^2 + 2u_{n-1}^2) dx \\
&= \frac{h}{2} \sum_{n=1}^N \int_\Omega (-u_n^2 + u_{n-1}^2) dx = \frac{h}{2} \int_\Omega (u_0^2 - u_N^2) dx \\
&\leq \frac{h}{2} \|u_0\|^2_{L^2(\Omega)}.
\end{aligned}$$

In the same way we also get

$$\|\nabla u^h\|^2_{L^2(Q_T)} - \|\nabla \overline{u}^h\|^2_{L^2(Q_T)} \leq \frac{h}{2} \|\nabla u_0\|^2_{L^2(Q_T)}.$$

Finally, from Poincare's inequality we know that there is a universal constant C_P so that

$$\|u^h\|_{L^2(Q_T)} \le C_P \|\nabla u^h\|_{L^2(Q_T)} \text{ for all } h \in (0,1). \tag{3.14}$$

We have obtained some results for future use. The results of the following Lemma rely only on the interpolations (3.7) and (3.6). The results are also independent of the problem under consideration and a fact frequently used later on.

Lemma 3. *Let $\overline{u}^h$ and u^h be defined by (3.7) and (3.6). Then the following relations hold.*

$$\|\overline{u}^h - u^h\|_{L^2(\Omega)} \le h\|u_t^h\|_{L^2(\Omega)} \text{ for a.e. } t \in (0,T), \tag{3.15}$$

$$\|u^h\|^2_{L^2(Q_T)} \le \|\overline{u}^h\|^2_{L^2(Q_T)} + \frac{h}{2}\|u_0\|^2_{L^2(\Omega)}, \tag{3.16}$$

$$\|\nabla u^h\|^2_{L^2(Q_T)} \le \|\nabla \overline{u}^h\|^2_{L^2(Q_T)} + \frac{h}{2}\|\nabla u_0\|^2_{L^2(\Omega)}. \tag{3.17}$$

Now, (3.11), (3.17) and (3.14) imply that u^h is uniformly bounded in $H^1(Q_T)$. Therefore, there is a weakly convergent subseguence in $H^1(Q_T)$ and, by Rellich theorem, a strongly converging subsequence in $L^2(Q_T)$. Let us denote the cluster function as u:

$$u^h \rightharpoonup u \text{ weakly in } H^1(Q_T) \tag{3.18}$$

Because of (3.13), $U = u_t$ holds almost everywhere. Moreover, from (3.12) for any $\varphi \in C_0^\infty(Q_T)$

$$\int_0^T \int_\Omega \Big(\frac{\partial \overline{u}^h}{\partial x_i} - \frac{\partial u^h}{\partial x_i}\Big)\varphi dxdt \to \int_0^T \int_\Omega \big(v_i - \frac{\partial u^h}{\partial x_i}\big)\varphi dxdt \text{ as } h \to 0+,$$

while at the same time

$$\int_0^T \int_\Omega \Big(\frac{\partial \overline{u}^h}{\partial x_i} - \frac{\partial u^h}{\partial x_i}\Big)\varphi dxdt = -\int_0^T \int_\Omega (\overline{u}^h - u^h)\frac{\partial \varphi}{\partial x_i} dxdt \to 0 \text{ as } h \to 0+,$$

by (3.15). This means that $\mathbf{v} = \nabla u$ almost everywhere in Q_T.
We have shown in this way that there is a function $u \in H^1(Q_T)$, such that

$$\nabla \overline{u}^h \rightharpoonup \nabla u \text{ in } (L^2(Q_T)^m) \tag{3.19}$$

$$u_t^h \rightharpoonup u_t \text{ in } L^2(Q_T) \tag{3.20}$$

Now, we can pass to limit in (3.10) as $h \to 0+$. We shall, for the time being, consider a test function φ belonging to $C_0^\infty([0,T] \times \Omega)$. To begin with, we have

$$\lim_{h \longrightarrow 0} \int_h^T \int_\Omega \nabla \overline{u}^h \nabla \varphi dx dt \tag{3.21}$$

$$= \lim_{h \longrightarrow 0} \int_0^T \int_\Omega \nabla \overline{u}^h \nabla \varphi dx dt - \lim_{h \longrightarrow 0} \int_0^h \int_\Omega \nabla \overline{u}^h \nabla \varphi dx dt \tag{3.22}$$

$$= \int_0^T \int_\Omega \nabla u \nabla \varphi dx dt \tag{3.23}$$

because the boundeness (3.11) of $\nabla \overline{u}^h$:

$$\begin{aligned} \Big| \int_0^h \int_\Omega \nabla \overline{u}^h \nabla \varphi dx dt \Big| &\leq \int_0^h \left(\int_\Omega |\nabla \overline{u}^h|^2 dx \right)^{1/2} \left(\int_\Omega |\nabla \varphi|^2 dx \right)^{1/2} dt \\ &\leq \int_0^h \sqrt{C_E} C dt = Ch \longrightarrow 0. \quad \text{as } h \to 0+. \end{aligned}$$

Moreover, for the first part of (3.10) we have:

$$\begin{aligned} & \int_h^T \int_\Omega \frac{u_t^h(t) - u_t^h(t-h)}{h} \varphi dx dt \\ = & \int_h^T \int_\Omega \frac{u_t^h(t)}{h} \varphi(t) dx dt - \int_0^{T-h} \int_\Omega \frac{u_t^h(t)}{h} \varphi(t+h) dx dt \\ = & \int_0^T \int_\Omega -\frac{u_t^h(t)}{h} (\varphi(t+h) - \varphi(t)) dx dt - \int_0^h \int_\Omega \frac{u_t^h(t)}{h} \varphi(t) dx dt \\ + & \int_{T-h}^T \int_\Omega \frac{u_t^h(t)}{h} \varphi(t+h) dx dt \end{aligned} \tag{3.24}$$

Such that for $h \longrightarrow 0$, by using integration by part, we obtain:

$$\lim_{h \longrightarrow 0} \int_h^T \int_\Omega \frac{u_t^h(t) - u_t^h(t-h)}{h} \varphi dx dt = \int_0^T \int_\Omega -u_t(t) \varphi_t(t) dx dt - \int_\Omega v_0 \varphi(0) dx \tag{3.25}$$

The convergence is deduced from the following facts:

1. in the first term of (3.24), u_t^h converges weakly and $(\varphi(t) - \varphi(t+h))/h$ converges strongly in $L^2(Q_T)$;

2. in the second term, $u_t^h = (u_1 - u_0)/h = v_0$ for $t \in (0, h)$;

3. in the third term, $\varphi(t+h) = 0$ for $t \in (T-h, T)$;

Finally, we get that:

$$\int_0^T \int_\Omega (-u_t(t)\varphi_t(t) + \nabla u \nabla \varphi) dx dt - \int_\Omega v_0 \varphi(0, x) dx = 0 \quad \forall \varphi \in C_0^\infty([0, T] \times \Omega) \tag{3.26}$$

Noting that the space of functions from $H^1(Q_T)$ with zero trace on $(\{0\} \times \Omega) \cup ([0, T] \times \partial\Omega)$ is a closed linear subspace of $H^1(Q_T)$ and, therefore, weakly closed by Mazur's theorem, we conclude by (3.18) that u belongs to this space. Consequently, u satisfies boundary condition (3.2) and initial condition (3.3) in the sense of traces. We remark that the convergence of traces follows also from the compactness of the trace operator $T : H^1(\Omega) \to L^2(\partial\Omega)$. Moreover, from [8] it follow that u, as a function from $H^1(0, T; L^2(\Omega))$, belong to $C([0, T]; L^2(\Omega))$. Thus, the initial condition (3.3) is satisfied even in the strong sense.
To summarize, we have proved by the discrete Morse flow method that there exist a weak solution $u \in H^1(Q_t)$ to problem (3.1)-(3.4) in the sense of (3.26), satisfying boundary and initial condition (3.2),(3.3) in the sense of traces.

3.2 The extensions of the DMF method

The DMF method can be naturally applied to problems with volume-constraint and free-boundary problems [15].
For hyperbolic problem with volume-constraint, we cite a result from [20]

Theorem 1. *Let us consider the following hyperbolic problem:*

$$\begin{aligned} u_{tt}(t, x) &= \Delta u(t, x) + \lambda(u), \quad (t, x) \in \Omega_T = (0, T) \times \Omega, && (3.27) \\ u(t, x) &= 0, \quad (t, x) \in (0, T) \times \partial\Omega, && (3.28) \\ u(0, x) &= u_0(x), \quad x \in \Omega, && (3.29) \\ u_t(0, x) &= v_0(x), \quad x \in \Omega. && (3.30) \end{aligned}$$

where $\lambda(u) = \frac{1}{V} \int_\Omega (u_{tt} u + |\nabla u|^2) dx$.
Let $T > 0$ *and* Ω *be a bounded domain in* $\mathbf{R}^m$ *with Lipschitz continuous boundary* $\partial\Omega$. *We assume that* $g \in L^2(\partial\Omega)$ *but put here* $g = 0$ *for simplicity.*

Further u_0, v_0 belong to $H^1(\Omega)$ satisfy the compatibility conditions $u_0(x) = g(x), v_0(x) = 0$ for $x \in \partial\Omega$ and $\int_\Omega u_0 dx = V, \int_\Omega v_0 dx = 0$. Then there is a weak solution $u \in H^1(0,T;L^2(\Omega)) \cap L^\infty(0,T;H_0^1(\Omega))$ satisfying the condition of constant volume, $u(0) = u_0$ and the following identity for all test function $\varphi \in C_0^\infty([0,T] \times \Omega)$ with $\Phi = \int_\Omega \varphi dx$

$$\int_0^T \int_\Omega (-u_t \varphi_t + \nabla u \nabla \varphi) dxdt - \int_\Omega v_0 \varphi(0) dx$$
$$= \frac{1}{V} \int_0^T \int_\Omega (-u_t (u\Phi)_t + |\nabla u|^2 \Phi) dxdt - \frac{1}{V} \int_\Omega u_0 v_0 \Phi(0) dx.$$

For a volume-constrained free boundary hyperbolic equation in one space dimension we cite a result from [17]

Theorem 2. *Let us consider the following hyperbolic problem:*

$$\chi_{u>0} u_{tt} = \Delta u - f(u) + \lambda \chi_{u>0}(u), \quad (t,x) \in \Omega_T = (0,T) \times \Omega, \tag{3.31}$$
$$u(t,x) = 0, \quad (t,x) \in (0,T) \times \partial\Omega, \tag{3.32}$$
$$u(0,x) = u_0(x), \quad x \in \Omega, \tag{3.33}$$
$$u_t(0,x) = v_0(x), \quad x \in \Omega. \tag{3.34}$$

where $\lambda(u) = \frac{1}{V} \int_\Omega (u_{tt} u + f(u) u + |\nabla u|^2) dx$.
Let $\Omega \subset \mathbf{R}$ be a domain with Lipschitz boundary and $T > 0$ a given final time. Assume that $f(t,x,u)$ is continuous in the variable u and satisfies $|f(t,x,u)| \leq C_f(u) + \Gamma(t,x)$ for some small constant C_f and a nonnegative $\Gamma \in L^2((0,T) \times \Omega)$. Further, assume that initial data u_0 and v_0 belong to $H_0^1(\Omega)$ satisfying the compatibility conditions $\int_\Omega u_0 dx = V, \int_\Omega v_0 dx = 0$. Then there exists a weak solution in the following sense.
A function $u \in H^1(0,T;L^2(\Omega)) \cap L^\infty(0,T;H_0^1(\Omega))$ is called a weak solution if $u(0,x) = u_0$, if $u = 0$ outside $\{u > 0\}$ and if the following identity holds for all $\varphi(t,x) \in C_0^\infty([0,T] \times \Omega \cap \{u > 0\})$ and an arbitrary $\tilde{u}(t,x) \in C_0^\infty([0,T] \times \Omega \cap \{u > 0\})$ satisfying $\int_\Omega \tilde{u}(t,x) dx = V$:

$$\int_0^T \int_\Omega (-u_t \varphi_t + \nabla u \nabla \varphi + f(u)\varphi) dxdt - \int_\Omega v_0 \varphi(0) dx$$
$$= \frac{1}{V} \int_0^T \int_\Omega (-u_t (\tilde{u}\Phi)_t + (\nabla u \nabla \tilde{u} + \tilde{u} f(u) \Phi) dxdt - \frac{1}{V} \int_\Omega \tilde{u}_0 v_0 \Phi(0) dx.$$

where $\Phi(t)$ denotes $\int_\Omega \varphi(t,x) dx$ and $\tilde{u}_0 = \tilde{u}(0,x)$.

Chapter 4

Smoothed particle hydrodynamics method

4.1 Introduction

Smoothed particle hydrodynamics (SPH) was invented to simulate astrophysical phenomena in astrophysics. This method has been widely studied and extended for applications to problems of continuum in solid and fluid mechanics [12]. The main feature of SPH method is to replace the equations of fluid dynamics by equations for particles. In this chapter, we shall show how a continuous field can be mapped on to a series of discrete particles. Then, we show how derivatives may be calculated.

4.2 Fundamental formulation of SPH

In order to derive the formulation of SPH, we consider two steps. The first step is the integral representation or kernel approximation of field functions. The second one is the particle approximation.

4.2.1 Kernel approximation

To obtain kernel approximation of a (scalar) function $f(\boldsymbol{r})$, the trivial identity is considered the starting point

$$f(\boldsymbol{r}) = \int_{\Omega} f(\boldsymbol{r'})\delta(\boldsymbol{r} - \boldsymbol{r'})d\boldsymbol{r'}, \tag{4.1}$$

$f(\boldsymbol{r})$ denotes a function of position vector $\boldsymbol{r}$, $\delta(\boldsymbol{r}-\boldsymbol{r'})$ is the Dirac delta function, and Ω is the volume of the integral that contain $\boldsymbol{r}$.
If we replace Delta function by a smoothing function $W(\boldsymbol{r}-\boldsymbol{r'},h)$, the kernel approximation of $f(\boldsymbol{r})$ is given by

$$< f(\boldsymbol{r}) >= \int_{\Omega} f(\boldsymbol{r'})W(\boldsymbol{r}-\boldsymbol{r'},h)d\boldsymbol{r'}. \tag{4.2}$$

The smoothing function W is usually chosen to be an even function. It should satisfy a number conditions, such as

The normalization condition:

$$\int_{\Omega} W(\boldsymbol{r}-\boldsymbol{r'},h)d\boldsymbol{r}' = 1, \tag{4.3}$$

Delta function property:

$$\lim_{h\to 0} W(\boldsymbol{r}-\boldsymbol{r'},h)d\boldsymbol{r'} = \delta(\boldsymbol{r}-\boldsymbol{r'}) \tag{4.4}$$

Compact condition:

$$W(\boldsymbol{r}-\boldsymbol{r'},h) = 0 \tag{4.5}$$

when $|\boldsymbol{r}-\boldsymbol{r'}| > \kappa h$ where κ is a constant related to smoothing function for point at $\boldsymbol{r}$, and defines the effective (non-zero) area of the smoothing function. This effective area is called the support domain for the smoothing function of point $\boldsymbol{r}$ (or the support domain of that point).

Using the Taylor series expansion of $f(\boldsymbol{r'})$ around $\boldsymbol{r'}$, where $f(\boldsymbol{r})$ is differentiable, we obtain following relation [12]:

$$< f(\boldsymbol{r}) >= f(\boldsymbol{r}) + O((\boldsymbol{r}'-\boldsymbol{r})^2) \tag{4.6}$$

Thus, the kernel approximation of a function is of second order accuracy in SPH method.

The gradient of a scalar function can be naturally calculated by taking the spatial derivative of equation (4.2):

$$< \nabla f(\boldsymbol{r}) >= \int_{\Omega} \left[\nabla' f(\boldsymbol{r'})\right] W(\boldsymbol{r}-\boldsymbol{r'},h)d\boldsymbol{r'}. \tag{4.7}$$

where ∇ and ∇' are gradients with respect to $\boldsymbol{r}$ and $\boldsymbol{r}'$, respectively. When we ignore the surface term, integrating by parts of (4.7) we obtain

$$< \nabla f(\boldsymbol{r}) >= \int_{\Omega} f(\boldsymbol{r'}) \nabla W(\boldsymbol{r} - \boldsymbol{r'}, h) d\boldsymbol{r'}. \tag{4.8}$$

Similarly, the kernel approximation of the derivative of a vector field $f(\boldsymbol{r})$ is given by

$$< \nabla . f(\boldsymbol{r}) >= \int_{\Omega} f(\boldsymbol{r'}) . \nabla W(\boldsymbol{r} - \boldsymbol{r'}, h) d\boldsymbol{r'}. \tag{4.9}$$

4.2.2 Particle approximation

The continuous integral representations can be converted to discretized forms of summation over all the particles in the support domain. This process is carried out as follows.

At position j, we use the finite volume of the particle $\triangle V_j$ to replace the infinitesimal volume $d\boldsymbol{r'}$, and mass of particle at this point is given by $m_j = \triangle V_j \rho_j$ where ρ_j is the density of particle j. Thus,

$$\begin{aligned} < f(\boldsymbol{r}) > &= \int_{\Omega} f(\boldsymbol{r'}) W(\boldsymbol{r} - \boldsymbol{r'}, h) d\boldsymbol{r'} \\ &\simeq \sum_j f(\boldsymbol{r}_j) W(\boldsymbol{r} - \boldsymbol{r}_j, h) \triangle V_j \\ &= \sum_j \frac{m_j}{\rho_j} f(\boldsymbol{r}_j) W(\boldsymbol{r} - \boldsymbol{r}_j, h) \end{aligned}$$

or

$$< f(\boldsymbol{r}) >= \sum_j \frac{m_j}{\rho_j} f(\boldsymbol{r}_j) W(\boldsymbol{r} - \boldsymbol{r}_j, h) \tag{4.10}$$

The particle approximation for a function at particle i can finally be written as

$$< f(\boldsymbol{r}_i) >= \sum_j \frac{m_j}{\rho_j} f(\boldsymbol{r}_j) W_{ij} \tag{4.11}$$

where

$$W_{ij} = W(\boldsymbol{r}_i - \boldsymbol{r}_j, h)$$

By using the same way, the particle approximation for the spatial derivative of the (scalar) function is

$$< \nabla f(\boldsymbol{r}) >= \sum_j \frac{m_j}{\rho_j} f(\boldsymbol{r}_j) \nabla W(\boldsymbol{r} - \boldsymbol{r}_j, h) \tag{4.12}$$

To obtain higher accuracy, the particle approximation would be done by writing [9]:

$$\rho \nabla A = \nabla(\rho A) - A \nabla \rho$$

In summary, the particle approximation for the spatial derivative of the function at particle i can finally be written as

$$< \nabla f(\boldsymbol{r}_i) >= \frac{1}{\rho_i} \sum_j m_j [f(\boldsymbol{r}_i) - f(\boldsymbol{r}_j)] \nabla_i W_{ij} \tag{4.13}$$

where

$$\nabla_i W_{ij} = \frac{\boldsymbol{r}_i - \boldsymbol{r}_j}{r_{ij}} \frac{\partial W_{ij}}{\partial r_{ij}} = \frac{\boldsymbol{r}_{ij}}{r_{ij}} \frac{\partial W_{ij}}{\partial r_{ij}}$$

In the case of vector field, the particle approximation for the spatial derivative at particle i can be given by:

$$< \nabla . f(\boldsymbol{r}_i) >= \frac{1}{\rho_i} \sum_j m_j [f(\boldsymbol{r}_i) - f(\boldsymbol{r}_j)] . \nabla_i W_{ij} \tag{4.14}$$

4.2.3 Smoothing Kernels

There are many different commonly used smoothing functions that have been implemented in SPH method. In this study we use cubic spline kernel which is defined as

$$W(r,h) = \frac{1}{\pi h^3} \begin{cases} 1 - 1.5x^2 + 0.75x^3, & \text{if } 0 \leq x < 1. \\ 0.25(2-x)^3, & \text{if } 1 \leq x \leq 2 \\ 0, & \text{if } 2 \leq x \end{cases} \tag{4.15}$$

where $x = \frac{r}{h}$.

The gradient of the kernel is well defined for all values of x, such that

$$\frac{\partial W(r,h)}{\partial r} = \frac{1}{\pi h^4} \begin{cases} -3x + 2.25x^2, & \text{if } 0 \leq x < 1. \\ -0.75(2-x)^2, & \text{if } 1 \leq x \leq 2 \\ 0, & \text{if } 2 \leq x \end{cases} \tag{4.16}$$

$$\nabla W(\boldsymbol{r}, h) = \frac{\boldsymbol{r}}{r} \frac{\partial W(r,h)}{\partial r}, r = |\boldsymbol{r}|$$

4.3 SPH Euler equations

In this study, The governing equations of the fluid are given as (Euler equations):

Momentum equation

$$\frac{D\boldsymbol{v}}{Dt} = -\frac{1}{\rho}\nabla P + \boldsymbol{g}, \tag{4.17}$$

Continuity equation

$$\frac{D\rho}{Dt} = -\rho\nabla.\boldsymbol{v} \tag{4.18}$$

Equation of state

$$P = P(\rho, c, \rho_0) \tag{4.19}$$

where $\frac{D}{Dt} = \frac{\partial}{\partial t} + \boldsymbol{v}.\nabla$ is material derivative, $\boldsymbol{v}$ is velocity, ρ is density, $\boldsymbol{g}$ is gravitation. We assume that c and ρ_0 are given.

In this section, we shall approximate density, velocity under particle form based on above particle approximations.

4.3.1 The momentum equation

Using the equation (4.13), the pressure gradient could be estimated by using

$$\rho_i\nabla P_i = \sum_j m_j(P_i - P_j)\nabla_i W_{ij}, \tag{4.20}$$

and this has the disadvantage that the linear and angular momentum are not conserved exactly. In this case, it is better to symmetrize the pressure gradient term by rewriting $\nabla P/\rho$ according to [9]:

$$\frac{\nabla P}{\rho} = \nabla\Big(\frac{P}{\rho}\Big) + \frac{P}{\rho^2}\nabla\rho$$

The momentum equation for particle i becomes

$$\frac{D\boldsymbol{v}_i}{Dt} = -\sum_j m_j\Big(\frac{P_i}{\rho_i^2} + \frac{P_j}{\rho_j^2}\Big)\nabla_i W_{ij} + \boldsymbol{g}_i \tag{4.21}$$

In order to improve the numerical stability, an artificial viscosity was proposed by Monaghan [11] and is given by

$$\Pi_{ij} = \begin{cases} -\alpha\mu_{ij}\frac{c_i+c_j}{\rho_i+\rho_j}, & \text{if } (\boldsymbol{v}_i - \boldsymbol{v}_j)(\boldsymbol{r}_i - \boldsymbol{r}_j) < 0. \\ 0, & \text{otherwise} \end{cases} \tag{4.22}$$

where $\mu_{ij} = \frac{(\boldsymbol{v}_i-\boldsymbol{v}_j).(\boldsymbol{r}_i-\boldsymbol{r}_j)}{|\boldsymbol{r}_i-\boldsymbol{r}_j|^2+\varepsilon h^2}$, c_k is the speed of sound which also appears in the state equation, $\varepsilon = 0.01, \alpha = 0.01$

Thus, the stabilized discrete momentum equations is described

$$\frac{D\boldsymbol{v}_i}{Dt} = -\sum_j m_j \left(\frac{P_i}{\rho_i^2} + \frac{P_j}{\rho_j^2} + \Pi_{ij}\right)\nabla W_{ij} + \boldsymbol{g}_i \tag{4.23}$$

4.3.2 Conservation of Mass

From equation (4.14), the divergence of velocity can be approximated following

$$\rho\nabla.\boldsymbol{v}_i = \sum_j m_j \boldsymbol{v}_{ij}.\nabla W_{ij} \tag{4.24}$$

where $\boldsymbol{v}_{ij} = \boldsymbol{v}_i - \boldsymbol{v}_j$.

Thus, the continuity equation can be replaced by

$$\frac{D\rho_i}{Dt} = \sum_j m_j \boldsymbol{v}_{ij}.\nabla W_{ij} \tag{4.25}$$

4.3.3 Particle positions

The governing equation of the position of a particle i at each time step is,

$$\frac{dr_i}{dt} = u_i,$$

where r_i is the position of particle i. There is also XSPH variant which consider artificial compressibility to incompresible flows. In the XSPH, the particle move in the following way,

$$\frac{dr_i}{dt} = u_i - \varepsilon\sum_j \frac{m_j}{\rho_j} u_{ij} W_{ij},$$

where ε is a constant in the ranging $0 \leq \varepsilon \leq 1.0$

4.3.4 Equation of State

There are many forms that relate to density and pressure. In the present implementation, the equation of state relates the pressure in fluids following

$$P = c^2(\rho - \rho_0),$$

where P is the pressure, c is artificial sound speed, and ρ_0 is reference density.

4.3.5 Boundary conditions

For a boundary and fluid particle separated by a distance $r = |\boldsymbol{r}|$, the force per unit mass $f(\boldsymbol{r})$ has the Lennard-Jones form [10]

$$f(\boldsymbol{r}) = \begin{cases} D\left[\left(\frac{r_0}{r}\right)^m - \left(\frac{r_0}{r}\right)^n\right]\frac{\boldsymbol{r}}{r^2}, & \text{if } r < r_0, \\ 0, & \text{otherwise} \end{cases} \tag{4.26}$$

The constant m and n must satisfy the condition $m > n$. In this work, we assign $m = 4, n = 2$ and r_0 is taken to be the initial spacing between the particles. For the last constant D, we chose $D = 0.01$.

4.3.6 Surface tension

Current surface tension models are commonly based on a color value c_i. All particles of a phase have the same color value and color values are interpolated according to

$$c_i = \sum_j \frac{m_j}{\rho_j} W_{ij}$$

The surface normal is calculated as

$$\boldsymbol{n}_i = \nabla c_i = \sum_j \frac{m_j}{\rho_j} \nabla W_{ij}$$

where $|\boldsymbol{n}_i| > 0$ only near and on the surface of the fluid.

The Gaussian curvature of the surface is measured following form

$$\kappa = -\frac{\nabla n}{|\boldsymbol{n}|} = -\frac{\nabla^2 c}{|\boldsymbol{n}|},$$

where the negation is necessary to get a positive curvature for convex fluid volume.

The surface tension traction, or external traction as opposed to internal traction that concerns stress fields, is force per unit area acting on a given location on the fluid's surface. The surface traction is defined as

$$t = \sigma\kappa\frac{\boldsymbol{n}}{|\boldsymbol{n}|},$$

and it should only be distributed to particles near and on the surface. As $|\boldsymbol{n}_i|$ becomes smaller when particle i is away from the surface, we can multiply the surface traction by a normalized scalar field $\delta_i = |\boldsymbol{n}_i|$. This will guarantee that the force density is spread to all potential particles, and ultimately results in the surface tension force,

$$f_i^{\text{surface}} = \delta_i t_i = \sigma\kappa_i\boldsymbol{n}_i = -\sigma\nabla^2 c_i\frac{\boldsymbol{n}}{|\boldsymbol{n}|}, \tag{4.27}$$

The surface tension force only applies to particles located near or on the liquid surface. This constraint is determined numerically as $\frac{\boldsymbol{n}}{|\boldsymbol{n}|}$, becomes numerical unstable when $|\boldsymbol{n}| \longrightarrow 0$. One way to prevent numerical problems when evaluating (4.27) for particle i, is compute f_i^{surface} only when

$$|\boldsymbol{n}_i| \geq l,$$

where $l > 0$ is some threshold relating to the particle concentration.

4.4 The Leap-Frog scheme

To simulate the fluid flow, each particle is advanced through time using a global fixed time step Δt. We have to compute the particle acceleration, and the new position is obtained from integrating the acceleration numerically. In this work, we use the leap-frog integration which is described as [12]:

At the end of the first time step (t_0), the change in density, and velocity are used to advance the density, and velocity at half a time step, while the particle position are advanced in a full time step

$$\begin{aligned}
t &= t_0 + \triangle t \\
\rho_i(t_0 + \triangle t/2) &= \rho_i(t_0) + \frac{\triangle t}{2} D\rho_i(t_0) \\
\boldsymbol{v}_i(t_0 + \triangle t/2) &= \boldsymbol{v}_i(t_0) + \frac{\triangle t}{2} D\boldsymbol{v}_i(t_0) \\
\boldsymbol{r}_i(t_0 + \triangle t) &= \boldsymbol{r}_i(t_0) + \triangle t \boldsymbol{v}_i(t_0 + \triangle t/2)
\end{aligned}$$

At the start of each subsequent time step, we predict the density, and velocity of each particle at half a time step.

$$\begin{aligned}
\rho_i(t) &= \rho_i(t - \triangle t/2) + \frac{\triangle t}{2} D\rho_i(t - \triangle t) \\
\boldsymbol{v}_i(t) &= \boldsymbol{v}_i(t - \triangle t/2) + \frac{\triangle t}{2} D\boldsymbol{v}_i(t - \triangle t)
\end{aligned}$$

At the end of the subsequent time step, the particle density, velocity and position are advanced in the standard leap-drop scheme

$$\begin{aligned}
t &= t + \triangle t \\
\rho_i(t + \triangle t/2) &= \rho_i(t - \triangle t/2) + \triangle t D\rho_i(t) \\
\boldsymbol{v}_i(t + \triangle t/2) &= \boldsymbol{v}_i(t - \triangle t/2) + \triangle t D\boldsymbol{v}_i(t) \\
\boldsymbol{r}_i(t + \triangle t) &= \boldsymbol{r}_i(t) + \triangle t \boldsymbol{v}_i(t + \triangle t/2)
\end{aligned}$$

Chapter 5

Numerical Computation

In this Chapter, we use finite element method to approximate functional $J_n(u)$. In order to find the minimizer of the functional, we use steepest descend method and bisection method.

Now we describe the main scheme to find minimizing sequence $\{u_n\}_{n=0}^{\infty}$ of functional $J_n(u)$. Generally, we consider hyperbolic with free boundary and volume-constraint. Other cases are described in Appendix.C.

Strong form:

$$\begin{aligned}
\sigma u_{tt}\chi_{u>0} &= \gamma\Delta u - R^2\chi_\varepsilon'(u) - \rho g u\chi_{u>0} + \lambda\chi_{u>0}, && \text{in } \Omega_T = (0,T)\times\Omega,\\
u(t,x,y) &= 0, && \text{on } (0,T)\times\partial\Omega,\\
u(0,x,y) &= u_0(x), && \text{in } \Omega,\\
u_t(0,x,y) &= v_0(x), && \text{in } \Omega.
\end{aligned}$$

here $\lambda = \int_\Omega(\sigma u_{tt}u + \gamma|\nabla u|^2 + \chi_\varepsilon(u) + \rho g u^2 + R^2\chi_\varepsilon(u))dx$

We consider the functional:

$$J_n(u) := \int_\Omega \Big(\sigma\frac{|u-2u_{n-1}+u_{n-2}|^2}{2h^2}\chi_{u>0}dx + \frac{\gamma}{2}|\nabla u|^2 + \frac{1}{2}\rho g u^2\chi_{u>0} + R^2\chi_\varepsilon(u)\Big)dx \tag{5.1}$$

in admissible set

$$K = \Big\{u \in H^1(\Omega), u|_{\partial\Omega} = 0, u > 0 \int_\Omega u\chi_{u>0}dx = V\Big\},$$

In order to get a minimizer $u_n, n = 1, 2, .., N$ of functional $J_n(u)$, we use the following minimizing algorithm:

1. Given the initial condition u_0 and v_0, set $u_{-1} = u_0 - hv_0$.

2. For $n = 0, 1, .., N$, determine u_{n+1} as follows:

   (a) $a^1 = u_n$

   (b) For $k = 1, 2, .., K_n$ *(maximum number of iterations)* repeat:

      i. compute the gradient $p_k = \nabla J_n(a^k)$,

      ii. search for the minimizer $\widetilde{a}^{k+1}$ of J_n in the direction $-p_k$,

      iii. set $\widetilde{a}^{k+1} = max(\widetilde{a}^{k+1}, 0)$

      iv. project a^{k+1} onto the volume-constraint hyperplane:

      $$a^{k+1} = Proj(\widetilde{a}_{k+1}),$$

      v. if convergence criterion is fulfilled, leave the cycle.

   (c) $u_{n+1} = a^{k+1}$

In this algorithm, $J_n(a^k)$ is approximated using finite element method for space discretization. Minimizers are determined by the steepest descent method, combined with a bisection method (step ii).

We divide domain Ω into N_e triangles $e_i, i = 1, 2, .., N_e$. Each triangle e has three nodes numbered $1, 2, 3$ with node coordinates $(x_1, y_1), (x_2, y_2), (x_3, y_3)$, and area A. In each triangle e, the terms are calculated following (see Appendix.A for more detail):

1. The first term
$$\int_e \frac{|u - 2u_{n-1} + u_{n-2}|^2}{2h^2} dx = (a_1^2 + a_2^2 + a_3^2 + a_1a_2 + a_2a_3 + a_3a_1)\frac{A}{6},$$
here $a_i = u(x_i, y_i) - 2u_{n-1}(x_i, y_i) + u_{n-2}(x_i, y_i), i = 1, 2, 3$

2. The third term $\int_e |\nabla u|^2 dx$ is calculated by using (Appendix.A.3).

3. The fourth term
$$\int_e u^2 dx = (a_1^2 + a_2^2 + a_3^2 + a_1a_2 + a_2a_3 + a_3a_1)\frac{A}{6},$$
here $a_i = u(x_i, y_i), i = 1, 2, 3$

4. The final term
$$\int_e \chi_\varepsilon(u)dx$$
This is the most complicated and important term. To calculate this one, we have to divide the triangle e into smaller triangle(s) following some rules (see Appendix.B for more details). Then this term is calculated on these smaller triangle(s).

Finally, the functional $J_n(u)$ can be approximated by

$$\begin{aligned} J_n(u) \simeq & \sum_i^{N_e} \int_{e_i} \sigma \frac{|u - 2u_{n-1} + u_{n-2}|^2}{2h^2} \chi_{u>0} dx + \sum_i^{N_e} \int_{e_i} \frac{1}{2} \rho g u^2 \chi_{u>0} dx \\ & + \frac{\gamma}{2} \sum_i^{N_e} \int_{e_i} |\nabla u|^2 dx + R^2 \sum_i^{N_e} \int_{e_i} \chi_\varepsilon(u) dx \end{aligned}$$

By using this main scheme and the others in Appendix.C, we present some examples which are calculated under Dirichlet boundary condition. In the first one, we consider the motion of a drop on plane (Figure. 5.1). This motion appears when we impart an initial velocity to the drop. The parameters in the equation (2.6) are given as

$$\sigma = 1, \gamma = 1, \rho = 1, R^2 = 1.2, \varepsilon = 0.04, h = 7.5 \times 10^{-4}$$

In the second example, we consider the behaviour of the film of a droplet pinned by the solid surface (Figure.5.2). In this case, the parameters in the equation (2.6) are given as

$$\sigma = 1, \gamma = 1, \rho = 1, R^2 = 1.2, \varepsilon = 0.03, h = 7.5 \times 10^{-4}$$

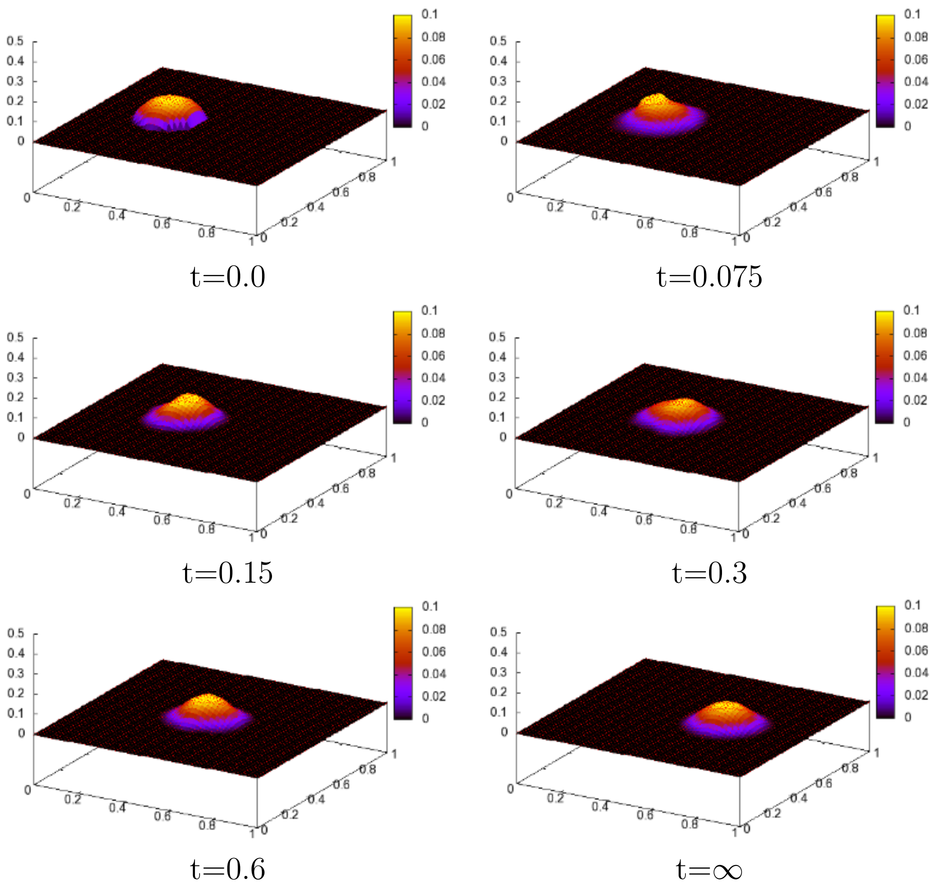

Figure 5.1: *A droplet moving on plane by initial velocity.*

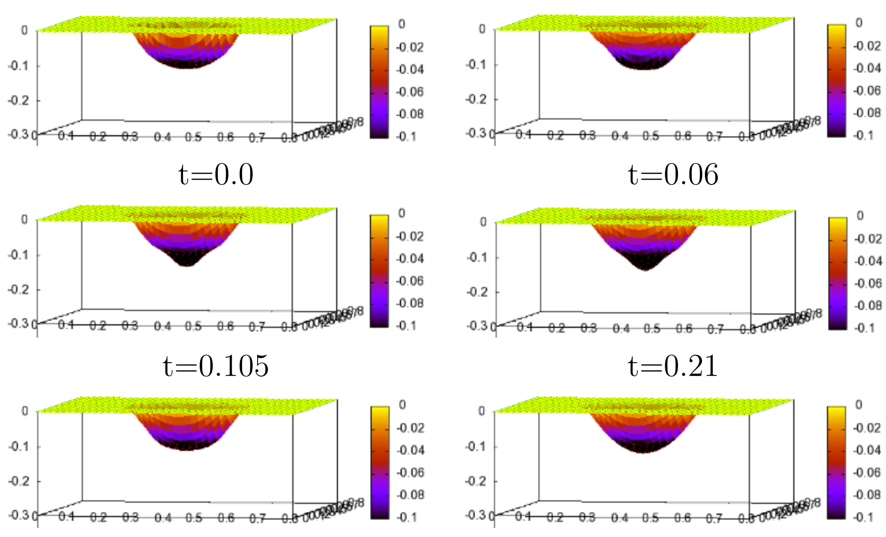

t=0.0 t=0.06

t=0.105 t=0.21

t=0.285 t=∞

Figure 5.2: *A droplet hanging on the plane.*

Chapter 6

Couple problem

6.0.1 The model of fluid

In this part, we examine the motion of fluid inside the film. This motion influences on the motion of the droplet as a whole. From the assumption, the domain of fluid flow at time t is given as:

$$\Omega_f(t) = \{(x, y, z) \in \mathbf{R}^3; (x, y) \in \Omega, z \in (0, u(t, x, y))\} \tag{6.1}$$

In this domain, we propose the motion of fluid following the equations:
Conservation of mass

$$\frac{D\rho}{Dt} + \rho\nabla.\boldsymbol{v} = 0, \text{ in } \cup_{t\in(0,T)} \Omega_f(t) \times \{t\}, \tag{6.2}$$

Conservation of momentum

$$\frac{D\boldsymbol{v}}{Dt} = -\frac{1}{\rho}\nabla P + \boldsymbol{g}, \text{ in } \cup_{t\in(0,T)} \Omega_f(t) \times \{t\}, \tag{6.3}$$

where $\boldsymbol{v}$ is the velocity, P is the pressure and $\boldsymbol{g}$ is the gravitation field vector. The pressure is determined by

$$P = c^2(\rho - \rho_0)$$

where c, ρ_0 are given.

6.0.2 The model of droplet motion

In order to achieve the model of the droplet motion, we consider an outer force against the surface - the pressure force pushing the film from the inside. The pressure force per unit area is written as $P\boldsymbol{n}$, where $\boldsymbol{n}$ is the unit outer normal vector of the surface, which is defined by

$$\boldsymbol{n} = \frac{\nabla F}{|\nabla F|} = \frac{1}{\sqrt{1+|\nabla u|^2}}(-u_x, -u_y, 1),$$

where $F(x, y, z) = z - u(x, y)$.

Therefore, $P(x, y, u, t)$ is the net force which is applied to the film [18]. In this case, the motion of the film follows the equation

$$\chi_{u>0}\sigma u_{tt} = \gamma_g \Delta u + P|_{z=u}\chi_{u>0} - R^2\chi'_\varepsilon(u) + \lambda\chi_{u>0}, \tag{6.4}$$

where

$$\lambda = \frac{1}{V}\int_\Omega \left(\gamma_g|\nabla u|^2 - uP|_{z=u} + R^2 u\chi'_\varepsilon(u) + \sigma u_{tt}u\right)dx.$$

Thus, a model of the droplet motion is given as

$$\chi_{u>0}\sigma u_{tt} = \gamma_g \Delta u + P|_{z=u}\chi_{u>0} - R^2\chi'_\varepsilon(u) + \lambda\chi_{u>0}, \text{ in } \Omega \times (0, T), \tag{6.5}$$

$$\frac{D\rho}{Dt} = -\rho\nabla.\boldsymbol{v}, \text{ in } \cup_{t\in(0,T)}\Omega_f(t) \times \{t\}, \tag{6.6}$$

$$\frac{D\boldsymbol{v}}{Dt} = -\frac{1}{\rho}\nabla P + \boldsymbol{g}, \text{ in } \cup_{t\in(0,T)}\Omega_f(t) \times \{t\}, \tag{6.7}$$

$$P = c^2(\rho - \rho_0), \text{ in } \cup_{t\in(0,T)}\Omega_f(t) \times \{t\}. \tag{6.8}$$

Taking the characteristic length L, characteristic time t_*, density ρ_0 and velocity v_*, we obtain the following nondimensional form of the equations:

$$\chi_{u>0}u_{tt} = \Gamma\Delta u + \Sigma P|_{z=u}\chi_{u>0} - \Pi\chi'_\varepsilon(u) + \lambda\chi_{u>0}, \text{ in } \Omega \times (0, T), \tag{6.9}$$

$$\frac{D\rho}{Dt} = -\rho\nabla \cdot \boldsymbol{v}, \text{ in } \cup_{t\in(0,T)}\Omega_f(t) \times \{t\}, \tag{6.10}$$

$$\frac{D\boldsymbol{v}}{Dt} = -\frac{1}{\rho}\nabla P + \kappa\boldsymbol{g}, \text{ in } \cup_{t\in(0,T)}\Omega_f(t) \times \{t\}, \tag{6.11}$$

$$P = c_s^2(\rho - 1), \text{ in } \cup_{t\in(0,T)}\Omega_f(t) \times \{t\}, \tag{6.12}$$

where

$$\Gamma = \frac{\gamma_g t_*^2}{\sigma L^2}, \Sigma = \frac{\rho_0 L}{\sigma}, \Pi = \frac{R^2 t_*^2}{\sigma L^2}, \kappa = \frac{t_*^2}{L}, c_s = \frac{c}{v_*}.$$

For the fluid flow, at $z = 0$ we impose the no-slip condition, $\boldsymbol{v} = \mathbf{0}$. Then

$$\left.\frac{\partial P}{\partial z}\right|_{z=0} = \kappa\rho\boldsymbol{g}\cdot\widehat{\boldsymbol{z}},$$

where $\widehat{\boldsymbol{z}} = (0, 0, 1)$.
At $z = u(x, y)$ we impose the free-slip condition. We consider velocity $\boldsymbol{v} = (\nu_1, \nu_2, \nu_3)$, and kinematic boundary condition is derived from $\mathrm{D}F/\mathrm{D}t = 0$:

$$u_t + \nu_1 u_x + \nu_2 u_y = \nu_3. \tag{6.13}$$

Thus we obtain

$$\boldsymbol{v}\cdot\boldsymbol{n} = \frac{u_t}{\sqrt{1+|\nabla u|^2}}. \tag{6.14}$$

From $\mathrm{D}^2F/\mathrm{D}t^2 = 0$, we can derive the following:

$$\left(\frac{\mathrm{D}\nu_3}{\mathrm{D}t} - u_x\frac{\mathrm{D}\nu_1}{\mathrm{D}t} - u_y\frac{\mathrm{D}\nu_2}{\mathrm{D}t}\right) = \frac{\mathrm{D}u_t}{\mathrm{D}t} + \nu_1\frac{\mathrm{D}u_x}{\mathrm{D}t} + \nu_2\frac{\mathrm{D}u_y}{\mathrm{D}t}.$$

Therefore,

$$\begin{aligned}
\boldsymbol{n}\cdot\frac{\mathrm{D}\boldsymbol{v}}{\mathrm{D}t} &= \frac{1}{\sqrt{1+|\nabla u|^2}}\left(\frac{\mathrm{D}u_t}{\mathrm{D}t} + \nu_1\frac{\mathrm{D}u_x}{\mathrm{D}t} + \nu_2\frac{\mathrm{D}u_y}{\mathrm{D}t}\right), \\
&= \frac{1}{\sqrt{1+|\nabla u|^2}}\left(u_{tt} + 2\nu_1 u_{xt} + 2\nu_2 u_{yt} + \nu_1^2 u_{xx} + 2\nu_1\nu_2 u_{xy} + \nu_2^2 u_{yy}\right).
\end{aligned}$$

From (6.11) and the above relation, we have

$$\begin{aligned}
\frac{\partial P}{\partial n} &= -\rho\boldsymbol{n}\cdot\frac{\mathrm{D}\boldsymbol{v}}{\mathrm{D}t} + \kappa\rho\boldsymbol{g}\cdot\boldsymbol{n}, \\
&= \frac{-\rho}{\sqrt{1+|\nabla u|^2}}\left(u_{tt} + 2\nu_1 u_{xt} + 2\nu_2 u_{yt} + \nu_1^2 u_{xx} + 2\nu_1\nu_2 u_{xy} + \nu_2^2 u_{yy}\right) + \kappa\rho\boldsymbol{g}\cdot\boldsymbol{n}, \\
&= -\frac{\rho}{\sqrt{1+|\nabla u|^2}}\left(\Gamma\Delta u + \Sigma P|_{z=u} - \Pi\chi_\varepsilon'(u) + \lambda\right) + \kappa\rho\boldsymbol{g}\cdot\boldsymbol{n} \\
&\quad -\frac{\rho}{\sqrt{1+|\nabla u|^2}}\left(2(\boldsymbol{v}\cdot\widehat{\boldsymbol{x}})u_{xt} + 2(\boldsymbol{v}\cdot\widehat{\boldsymbol{y}})u_{yt} + (\boldsymbol{v}\cdot\widehat{\boldsymbol{x}})^2 u_{xx} + 2(\boldsymbol{v}\cdot\widehat{\boldsymbol{x}})(\boldsymbol{v}\cdot\widehat{\boldsymbol{y}})u_{xy} + (\boldsymbol{v}\cdot\widehat{\boldsymbol{y}})^2 u_{yy}\right),
\end{aligned}$$

where $\widehat{\boldsymbol{x}} = (1, 0, 0), \widehat{\boldsymbol{y}} = (0, 1, 0)$.

In summary, a model of the droplet motion is given as

$$\chi_{u>0}u_{tt} = \Gamma\Delta u + \Sigma P|_{z=u}\chi_{u>0} - \Pi\chi'_\varepsilon(u) + \lambda\chi_{u>0}, \text{ in } \Omega\times(0,T), \tag{6.15}$$

$$\frac{D\rho}{Dt} = -\rho\nabla\cdot\boldsymbol{v}, \text{ in } \cup_{t\in(0,T)}\Omega_f(t)\times\{t\}, \tag{6.16}$$

$$\frac{D\boldsymbol{v}}{Dt} = -\frac{1}{\rho}\nabla P + \kappa\boldsymbol{g}, \text{ in } \cup_{t\in(0,T)}\Omega_f(t)\times\{t\}, \tag{6.17}$$

$$P = c_s^2(\rho-1), \text{ in } \cup_{t\in(0,T)}\Omega_f(t)\times\{t\}, \tag{6.18}$$

$$\boldsymbol{v} = 0, \frac{\partial P}{\partial z} = \kappa\rho\boldsymbol{g}\cdot\widehat{\boldsymbol{z}}, \text{ at } z=0 \tag{6.19}$$

$$\boldsymbol{v}\cdot\boldsymbol{n} = \frac{u_t}{\sqrt{1+|\nabla u|^2}}, \text{ at } z=u \tag{6.20}$$

$$\begin{aligned}\frac{\partial P}{\partial n}\Big|_{z=u} &= -\frac{\rho}{\sqrt{1+|\nabla u|^2}}\big(\Gamma\Delta u + \Sigma P|_{z=u} - \Pi\chi'_\varepsilon(u) + \lambda\big) + \kappa\rho\boldsymbol{g}\cdot\boldsymbol{n}\\ &\quad -\frac{\rho}{\sqrt{1+|\nabla u|^2}}\Big(2(\boldsymbol{v}\cdot\widehat{\boldsymbol{x}})u_{xt} + 2(\boldsymbol{v}\cdot\widehat{\boldsymbol{y}})u_{yt} + (\boldsymbol{v}\cdot\widehat{\boldsymbol{x}})^2u_{xx}\\ &\quad +2(\boldsymbol{v}\cdot\widehat{\boldsymbol{x}})(\boldsymbol{v}\cdot\widehat{\boldsymbol{y}})u_{xy} + (\boldsymbol{v}\cdot\widehat{\boldsymbol{y}})^2u_{yy}\Big).\end{aligned} \tag{6.21}$$

The whole system is solved by combining the discrete Morse flow with the SPH method. At each time level $t = nh$, we have the shape of the film u_n, the positions and velocities of fluid particles $\{\boldsymbol{x}_n^m\}_{m=1}^M, \{\boldsymbol{v}_n^m\}_{m=1}^M$, from which we can find the new shape u_{n+1} of the film, the new positions and velocities $\{\boldsymbol{x}_{n+1}^m\}_{m=1}^M, \{\boldsymbol{v}_{n+1}^m\}_{m=1}^M$ of the fluid particles as follows:

1. Predict the shape of the film u^* using the discrete Morse flow method without a pressure force.

2. Determine position $\boldsymbol{x}_{n+1}^m$, velocity $\boldsymbol{v}_{n+1}^m$, and pressure P_{n+1}^m in the region below u^*, using the SPH method.

3. Determine the new shape u_{n+1} of the film, using the discrete Morse flow method with the pressure force.

We use above procedure to simulate the motion of a droplet under inclined plane with angle $\alpha = 20°$ (Figure. 6.1). The domain $\Omega = (0,1)\times(0,0.6)$ is divided into 80×48 squares with $\Delta x = 1/80$ and each square is divided into two triangle elements. In addition, the parameters of equation (6.15) are given as

$$\Gamma = 1, \Sigma = 1, \Pi = 1.65, \varepsilon = 3.2\Delta x, h = 4\times10^{-4}, \kappa = 0.1, c_s = \sqrt{5}$$

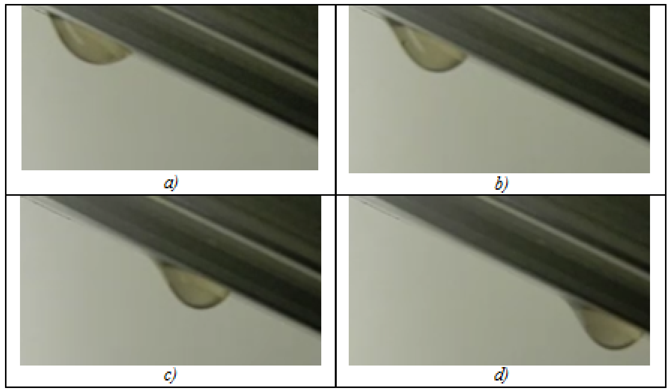

Figure 6.1: *A droplet lying under inclined plane (experiment).*

and the fluid inside the drop is represented by 1451 particles.

By observing the simulation results (Figure 6.2), it can be seen that the shape of droplet oscillates and the volume is preserved within the discretization error while the droplet moves. In addition, there are no particles moving out of the film during the motion. In other words, the number of particles representing the fluid is controlled well by the film during the motion. Judging from the obtained shapes of the droplet these results show a qualitative agreement with observations from the real experiments.

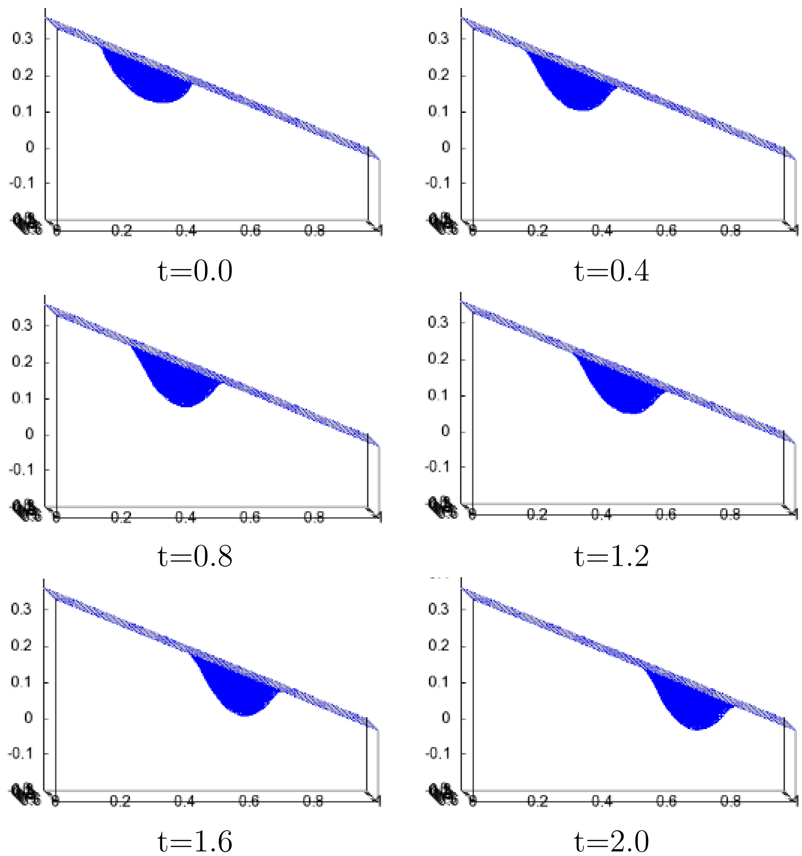

Figure 6.2: *A droplet lying under inclined plane (simulation).*

Chapter 7

Conclusion

We have derived the hyperbolic free boundary problem with volume conservation constraint based on examining the motion of the surface of a droplet on plane or inclined plane. An approximation solution of this problem has been designed using the discrete Morse flow method. This method induced good numerical results, the droplet oscillates and its volume is precisely preserved. We have also presented a couple model for the moving droplet by combining the above hyperbolic problem for the film with the Euler equations for fluid filling film. In this case, the film plays as the moving boundary of the fluid and it always fills on role. Numerical result shows qualitative agreement with observed fact. Our goal for future research is quantitative comparison for this model.

Appendix A

Finite element method

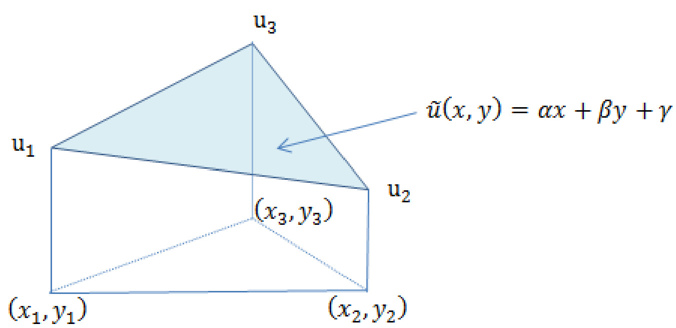

In the domain $\Omega \subset \mathbf{R}^2$. we consider a triangle element e with node number $1, 2, 3$. The node coordinates are $(x_1, y_1), (x_2, y_2), (x_3, y_3)$. On this triangle, we assume to have a planar variation $\tilde{u}(x, y)$:

$$\tilde{u}(x, y) = \alpha x + \beta y + \gamma$$

where α, β, γ are to be determined in terms of the values of $\tilde{u}(x, y)$ at the nodes $(x_1, y_1), (x_2, y_2), (x_3, y_3)$. We denote $u_i = \tilde{u}(x_i, y_i), i = 1, 2, 3$:

$$u_i = \alpha x_i + \beta y_i + \gamma \qquad (i = 1, 2, 3)$$

We have the matrix form

$$\begin{pmatrix} u_1 \\ u_2 \\ u_3 \end{pmatrix} = \begin{pmatrix} x_1 & y_1 & 1 \\ x_2 & y_2 & 1 \\ x_3 & y_3 & 1 \end{pmatrix} \begin{pmatrix} \alpha \\ \beta \\ \gamma \end{pmatrix}$$

We denote

$$D := \begin{vmatrix} x_1 & y_1 & 1 \\ x_2 & y_2 & 1 \\ x_3 & y_3 & 1 \end{vmatrix}$$

Because of $D \neq 0$ we can use Cramer's rule and obtain

$$\alpha = \frac{\begin{vmatrix} u_1 & y_1 & 1 \\ u_2 & y_2 & 1 \\ u_3 & y_3 & 1 \end{vmatrix}}{D}, \quad \beta = \frac{\begin{vmatrix} x_1 & u_1 & 1 \\ x_2 & u_2 & 1 \\ x_3 & u_3 & 1 \end{vmatrix}}{D}, \quad \gamma = \frac{\begin{vmatrix} x_1 & y_1 & u_1 \\ x_2 & y_2 & u_2 \\ x_3 & y_3 & u_3 \end{vmatrix}}{D}$$

If we denote, $(i, j, k) = (1, 2, 3), (2, 3, 1), (3, 1, 2)$ and

$$a_i := \frac{y_j - y_k}{D}, \quad b_i := \frac{x_k - x_j}{D}, \quad c_i := \frac{x_j y_k - x_k y_j}{D} \tag{A.1}$$

then we get

$$\begin{pmatrix} \alpha \\ \beta \\ \gamma \end{pmatrix} = \begin{pmatrix} a_1 & a_2 & a_3 \\ b_1 & b_2 & b_3 \\ c_1 & c_2 & c_3 \end{pmatrix} \begin{pmatrix} u_1 \\ u_2 \\ u_3 \end{pmatrix}$$

that is

$$\alpha = \sum_{i=1}^{3} a_i u_i, \quad \beta = \sum_{i=1}^{3} b_i u_i, \quad \gamma = \sum_{i=1}^{3} c_i u_i,$$

Thus

$$\tilde{u}(x, y) = \sum_{i=1}^{3} (a_i x + b_i y + c_i) u_i$$

We denote

$$\lambda_i(x, y) := a_i x + b_i y + c_i$$

then

$$\tilde{u}(x, y) = \sum_{i=1}^{3} \lambda_i u_i \tag{A.2}$$

here, $\lambda_1, \lambda_2, \lambda_3$ called shape functions.
Form this formula, we can find gradient of $\tilde{u}(x, y)$ following as

$$\frac{\partial \tilde{u}}{\partial x} = \sum_{i=1}^{3} \frac{\partial \lambda_i}{\partial x} u_i = \sum_{i=1}^{3} a_i u_i \tag{A.3}$$

$$\frac{\partial \tilde{u}}{\partial y} = \sum_{i=1}^{3} \frac{\partial \lambda_i}{\partial y} u_i = \sum_{i=1}^{3} b_i u_i \tag{A.4}$$

We also get some properties of shape functions

1. $\lambda_i(x_j, y_j) = \delta_{ij}$
2. $\lambda_1 + \lambda_2 + \lambda_3 = 1, \forall (x, y) \in e$.
3. $\int_e \lambda_i^2 dx = \frac{A}{6}, i = 1, 2, 3$ where A is the area of triangle element e.
4. $\int_e \lambda_i \lambda_j dx = \frac{A}{12}, i \neq j$

1) In fact,

$$\lambda_1(x_1, y_1) = a_1 x_1 + b_1 y_1 + c_1 = \frac{(y_2 - y_3)x_1 + (x_3 - x_2)y_1 + x_2 y_3 - x_3 y_2}{D} = 1.$$

$$\lambda_1(x_2, y_2) = a_1 x_2 + b_1 y_2 + c_1 = \frac{(y_2 - y_3)x_2 + (x_3 - x_2)y_2 + x_2 y_3 - x_3 y_2}{D} = 0.$$

$$\lambda_1(x_3, y_3) = a_1 x_3 + b_1 y_3 + c_1 = \frac{(y_2 - y_3)x_3 + (x_3 - x_2)y_3 + x_2 y_3 - x_3 y_2}{D} = 0.$$

For λ_2, λ_3 we show the same way.

2) In fact,

$$\begin{aligned} \lambda_1 + \lambda_2 + \lambda_3 &= (a_1 + a_2 + a_3)x + (b_1 + b_2 + b_3)y + (c_1 + c_2 + c_3) \\ &= \frac{0.x + 0.y + x_2 y_3 - x_3 y_2 + x_3 y_1 - x_1 y_3 + x_1 y_2 - x_2 y_1}{D} \\ &= 1. \end{aligned}$$

3) We consider a differential strip parallel to the side opposite node i in the triangle e. and we denote b is the length of the side opposite to node i and h is the height of the perpendicular from node i to the opposite side. If λ_i

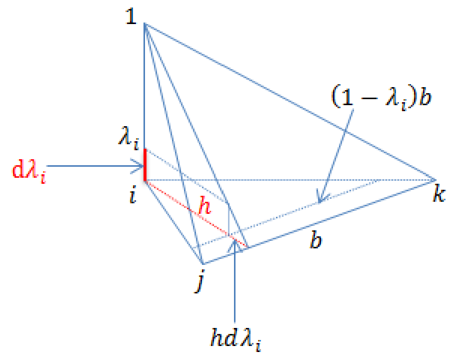

Figure A.1: Shape function.

change $d\lambda_i$, the width of strip is $hd\lambda_i$ and the length of the strip is $(1-\lambda_i)b$, (Figure A). So

$$\int_e \lambda_i^2 dx = \int_0^1 \lambda_i^2(1-\lambda_i)bhd\lambda_i = \frac{bh}{12} = \frac{A}{6}$$

4) We have

$$\int_e (\lambda_1^2 + \lambda_1\lambda_2 + \lambda_1\lambda_3)dx = \int_e \lambda_1 dx = \int_0^1 \lambda_1(1-\lambda_1)bhd\lambda_1 = \frac{bh}{6} = \frac{A}{3}$$

and

$$\int_e \lambda_1^2 dx = \frac{A}{6}$$

So

$$\int_e (\lambda_1\lambda_2 + \lambda_1\lambda_3)dx = \frac{A}{6}$$

Similarly, we also have

$$\int_e (\lambda_2\lambda_1 + \lambda_2\lambda_3)dx = \frac{A}{6}$$

$$\int_e (\lambda_3\lambda_1 + \lambda_3\lambda_2)dx = \frac{A}{6}$$

Thus

$$\int_e \lambda_i\lambda_j dx = \frac{A}{12}, i \neq j$$

Using these results can approximate

$$\begin{aligned}
\int_e u dx &= (u_1 + u_2 + u_3)\frac{A}{3}. \\
\int_e u^2 dx &= \int_e (\lambda_1 u_1 + \lambda_2 u_2 + \lambda_3 u_3)^2 dx \\
&= \int_e (\lambda_1^2 u_1^2 + \lambda_2^2 u_2^2 + \lambda_3^2 u_3^2 + 2\lambda_1\lambda_2 u_1 u_2 + 2\lambda_2\lambda_3 u_2 u_3 + 2\lambda_3\lambda_1 u_3 u_1) dx \\
&= (\frac{A}{6}u_1^2 + \frac{A}{6}u_2^2 + \frac{A}{6}u_3^2 + 2\frac{A}{12}u_1 u_2 + 2\frac{A}{12}u_2 u_3 + 2\frac{A}{12}u_3 u_1) \\
&= (u_1^2 + u_2^2 + u_3^2 + u_1 u_2 + u_2 u_3 + u_3 u_1)\frac{A}{6} \\
\int_e |u - u^*|^2 dx &= \int_e (\lambda_1(u_1 - u_1^*) + \lambda_2(u_2 - u_2^* + \lambda_3(u_3 - u_3^*))^2 dx \\
&= \int_e (\lambda_1^2 a^2 + \lambda_2^2 b^2 + \lambda_3^2 c^2 + 2\lambda_1\lambda_2 ab + 2\lambda_2\lambda_3 bc + 2\lambda_3\lambda_1 ca) dx \\
&= (\frac{A}{6}a^2 + \frac{A}{6}b^2 + \frac{A}{6}c^2 + 2\frac{A}{12}ab + 2\frac{A}{12}bc + 2\frac{A}{12}ca) \\
&= (a^2 + b^2 + c^2 + ab + bc + ca)\frac{A}{6}
\end{aligned}$$

where $a = u_1 - u_1^*, b = u_2 - u_2^*, c = u_3 - u_3^*$.

Appendix B

Characteristic function

This part we will explain how to calculate $E = \int_e \chi_\varepsilon(u)dx$ by using finite element method.

We assume a triangle element e with node coordinates $(x_1, y_1), (x_2, y_2), (x_3, y_3)$, and values of function $u(x, y)$ at these nodes are

$$u_1 = u(x_1, y_1), u_2 = u(x_2, y_2), u_3 = u(x_3, y_3).$$

We also denote $A_{(ijk)}$ is the area of triangle with three nodes i, j, k.
The main scheme is following the chart:

we arrange $u_i, i = 1, 2, 3$ so that $u_1 \leq u_2 \leq u_3$.

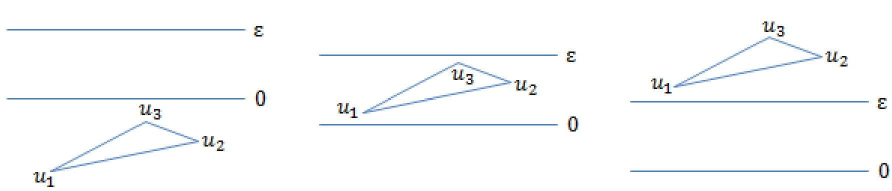

(a) (b) (c)

Figure B.1: Case 1, 2 and 3.

1. Case 1: If $u_3 \leq 0$ (Figure B (a)) then $E = 0$.
2. Case 2: If $0 \leq u_1$ and $u_3 \leq \varepsilon$ (B (b)) then $E = (u_1 + u_2 + u_3)\frac{A}{3}$.

3. Case 3: If $u_1 \geq \varepsilon$ (Figure B (c)) then $E = A$.
4. Case 4: If $u_1 \geq 0$ then we consider three cases $u_2 < \varepsilon, u_2 = \varepsilon$, and $u_2 > \varepsilon$,

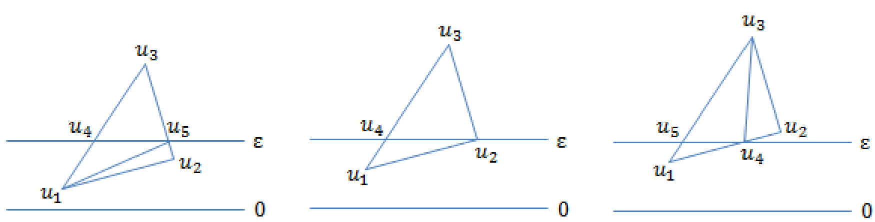

(a) (b) (c)

Figure B.2: Case 4, $0 \leq u_1 \leq u_2 \leq \varepsilon < u_3, u_1 < \varepsilon$

(a) If $u_2 < \varepsilon$ then e is divided into three small triangles (Figure B.2 (a)). Thus

$$E = \frac{u_1 + u_2 + u_5}{3} A_{(125)} + \frac{u_1 + u_4 + u_5}{3} A_{(145)} + A_{(453)}$$

(b) If $u_2 = \varepsilon$ then e is divided into two small triangles (Figure B.2 (b)). Thus

$$E = \frac{u_1 + u_2 + u_4}{3} A_{(124)} + A_{(423)}$$

(c) If $u_2 > \varepsilon$ then we divide e to three small triangles (Figure B.2 (c)). Thus

$$E = \frac{u_1 + u_4 + u_5}{3} A_{(145)} + A_{(453)} + A_{(423)}$$

5. Case 5: If $u_1 < 0$ then we consider three cases $u_2 \leq 0$, and $u_2 > 0$,

   (a) If $u_2 \leq 0$ then $E = \int_{(243)} \chi_\varepsilon(u)dx$ (Figure B.3)

      i. If $u_3 \leq \varepsilon$ then we use case 2 (Figure B.3 (a) and (c)).

      ii. If $u_3 > \varepsilon$ then we use case 4 (Figure B.3 (b) and (d)).

   (b) If $u_2 > 0$ then $E = \int_{(423)} \chi_\varepsilon(u)dx + \int_{(453)} \chi_\varepsilon(u)dx$ (Figure B.4)

      i. If $u_3 \leq \varepsilon$ then we use case 2 (Figure B.4 (a)).

      ii. If $u_3 > \varepsilon$ then we use case 4 (Figure B.4 (b),(c) and (d)).

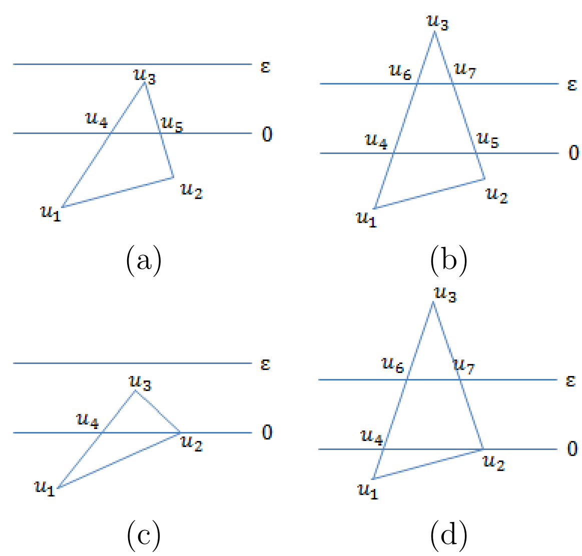

Figure B.3: Case 5, $u_1 < u_2 \leq 0 < u_3$.

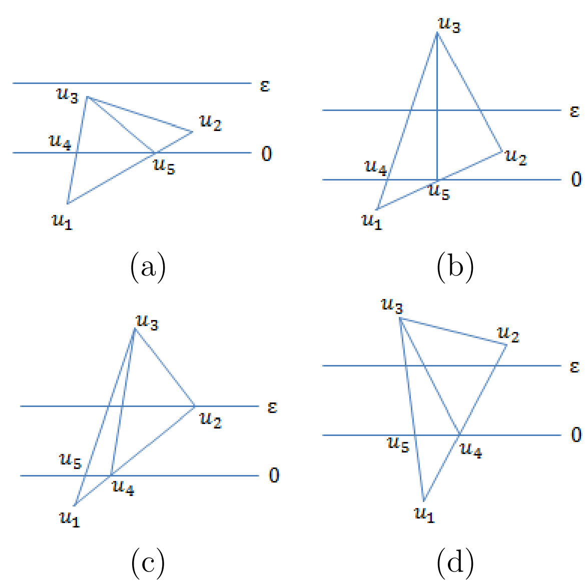

Figure B.4: Case 5, $u_1 < 0 < u_2 < u_3$.

Appendix C

Main scheme to find the minimizing sequence

In this part we consider four hyperbolic problems: Hyperbolic problem, hyperbolic with volume-constraint problem, hyperbolic with free boundary problem and hyperbolic with free boundary and volume-constraint problem. Depend on each problems we have to find the minimizing sequence $\{u_n\}_{n=0}^{\infty}$ of difference functional in difference admissible set K. Further, in our work we just consider Dirichlet boundary.

C.1 Hyperbolic problem

Strong form:

$$\begin{aligned}
u_{tt}(t,x,y) &= \Delta u(t,x,y), && \text{in } \Omega_T = (0,T)\times\Omega,\\
u(t,x,y) &= 0, && \text{on } (0,T)\times\partial\Omega,\\
u(0,x,y) &= u_0(x), && \text{in } \Omega,\\
u_t(0,x,y) &= v_0(x), && \text{in } \Omega.
\end{aligned}$$

The functional:

$$J_n(u) := \int_{\Omega}\Big(\frac{|u-2u_{n-1}+u_{n-2}|^2}{2h^2}dx + \frac{1}{2}|\nabla u|^2\Big)dx \tag{C.1}$$

Admissible set

$$K = \Big\{u \in H^1(\Omega), u|_{\partial\Omega} = 0\Big\},$$

1. Given the initial condition u_0 and v_0, set $u_{-1} = u_0 - hv_0$.
2. For $n = 0, 1, .., N$, determine u_{n+1} as follows:
   (a) $a^1 = u_n$
   (b) For $k = 1, 2, .., K_n$ *(maximum number of iterations)* repeat:
      i. compute the gradient $p_k = \nabla J_n(a^k)$,
      ii. search for the minimizer $\widetilde{a}^{k+1}$ of J_n in the direction $-p_k$,
      iii. if convergence criterion is fulfilled, leave the cycle.
   (c) $u_{n+1} = a^{k+1}$

C.2 Hyperbolic with volume-constraint

Strong form:

$$\begin{aligned} u_{tt}(t,x,y) &= \Delta u(t,x,y) + \lambda(t), && \text{in } \Omega_T = (0,T)\times\Omega, \\ u(t,x,y) &= 0, && \text{on } (0,T)\times\partial\Omega, \\ u(0,x,y) &= u_0(x), && \text{in } \Omega, \\ u_t(0,x,y) &= v_0(x), && \text{in } \Omega. \end{aligned}$$

here $\lambda(t) = \int_\Omega (u_{tt}u + |\nabla u|^2)dx$ The functional:

$$J_n(u) := \int_\Omega \Big(\frac{|u - 2u_{n-1} + u_{n-2}|^2}{2h^2} dx + \frac{1}{2}|\nabla u|^2 \Big) dx \tag{C.2}$$

Admissible set

$$K = \Big\{ u \in H^1(\Omega), u|_{\partial\Omega} = 0, \int_\Omega u dx = V \Big\},$$

The basic course of finding u_n is following chart

1. Given the initial condition u_0 and v_0, set $u_{-1} = u_0 - hv_0$.
2. For $n = 0, 1, .., N$, determine u_{n+1} as follows:
   (a) $a^1 = u_n$
   (b) For $k = 1, 2, .., K_n$ *(maximum number of iterations)* repeat:

i. compute the gradient $p_k = \nabla J_n(a^k)$,

ii. search for the minimizer $\widetilde{a}^{k+1}$ of J_n in the direction $-p_k$,

iii. project a^{k+1} onto the volume-constraint hyperplane:

$$a^{k+1} = Proj(\widetilde{a}_{k+1}),$$

iv. if convergence criterion is fulfilled, leave the cycle.

(c) $u_{n+1} = a^{k+1}$

C.3 Hyperbolic with free boundary problem

Strong form:

$$\begin{aligned}
\chi_{u>0} u_{tt}(t,x,y) &= \Delta u(t,x,y) + \chi'_{\varepsilon}(u) + \lambda(t)\chi_{u>0}, && \text{in } \Omega_T = (0,T)\times\Omega,\\
u(t,x,y) &= 0, && \text{on } (0,T)\times\partial\Omega,\\
u(0,x,y) &= u_0(x), && \text{in } \Omega,\\
u_t(0,x,y) &= v_0(x), && \text{in } \Omega.
\end{aligned}$$

here $\lambda(t) = \int_\Omega (u_{tt}u + |\nabla u|^2 + \chi_\varepsilon(u))dx$ The functional:

$$J_n(u) := \int_\Omega \Big(\frac{|u - 2u_{n-1} + u_{n-2}|^2}{2h^2} \chi_{u>0} dx + \frac{1}{2}|\nabla u|^2 + \chi_\varepsilon(u)\Big) dx \tag{C.3}$$

Admissible set

$$K = \Big\{ u \in H^1(\Omega), u|_{\partial\Omega} = 0, u > \varphi \Big\},$$

The basic course of finding u_n is following chart

1. Given the initial condition u_0 and v_0, set $u_{-1} = u_0 - hv_0$.
2. For $n = 0, 1, .., N$, determine u_{n+1} as follows:

(a) $a^1 = u_n$

(b) For $k = 1, 2, .., K_n$ *(maximum number of iterations)* repeat:

i. compute the gradient $p_k = \nabla J_n(a^k)$,

ii. search for the minimizer $\widetilde{a}^{k+1}$ of J_n in the direction $-p_k$,

iii. set $\widetilde{a}^{k+1} = max(\widetilde{a}^{k+1}, \varphi)$

iv. if convergence criterion is fulfilled, leave the cycle.

(c) $u_{n+1} = a^{k+1}$

Acknowledgement

From the bottom of my heart, I would like to express my honest gratitude and sincere appreciation to my academic supervisor, Professor Seiro Omata who has been supporting me not only in the research but also in daily life. He has guided me with the outstanding directions at the every stage of my study.

I am deeply grateful to Professor Karel Švadlenka and Professor Katsuyoshi Ohara for their valuable advice and kind help.

I also wish to express my deepest gratitude to Kanazawa University as well as all members of Student Affair, Japanese teachers who enthusiastically helped me since the beginning of my study and life in Kanazawa.

I am extremely thankful to Mr. Yukio Abe and Mr. Mi Tetuo, who kindly helped me since I started my new life in Japan. I also would like to extend my special thanks to my dear friends and laboratory colleagues who assisted me directly or indirectly in both my study and daily life. For those I could not name them all, and for this purpose let me appreciate them.

I would also like to express my gratitude to the Mekong Camau 120 Project, Mekong 1000 Project for their financial support during the entire period of my study.

I honestly express my deepest respect and extreme gratitude to my dear parents, my siblings, my wife and my sons. They were always supporting me and encouraging me with their best wish.

Bibliography

[1] N. Kikuchi, *An approach to the construction of Morse flows for variational functionals,* in "Nematics - Mathematical and Physical Aspects", ed.: J.-M. Coron, J.-M. Ghidaglia, F. Hélein, NATO Adv. Sci. Inst. Ser. C: Math. Phys. Sci. 332, Kluwer Acad. Publ., Dodrecht-Boston-London, 1991, pp. 775-786.

[2] K. Hoshino, N. Kikuchi, *On a construction of weak solutions to linear hyperbolic partial differential systems with the higher integrable gradients,* J. Math. Sci. 93, 199, pp. 636-652.

[3] H. Imai, K. Kikuchi, K. Nakane, S. Omata, T. Tachikawa, *A numerical approach to the asymptotic behavior of solutions of a one-dimensional hyperbolic free boundary problem,* JJIAM 18 (1), 2001, pp. 43-58.

[4] K. Kikuchi, S. Omata, *A free boundary problem for a one dimensional hyperbolic equation,* Adv. Math. Sci. Appl. 9 (2),1999, pp. 775-786.

[5] S. Omata, *A numerical method based on the discrete Morse semiflow related to parabolic and hyperbolic equation,* Nonlinear Analysis 30 (4), 2003, pp. 2181-2187.

[6] K. Švadlenka, S. Omata, *Construction of solutions to heat-type problems with volume constraint via the discrete Morse flow,* Funks. Ekvac. 50, 2007, pp. 261-285.

[7] S. Omata, M. Kazama, H. Nakagawa, *Variational approach to evolutionary free boundary problems,* Nonlinear Analysis, 71 (2009),pp. e1547-e1552.

[8] L.C.Evans, *Partial Differential Equations,* Graduate Studies in Mathematics, AMS, Province, Rhode Island, 1998.

[9] J.J. Monaghan, *Smoothed particle hydrodynamics,* Annu. Rev. Astron. Astrophys, 30, 1992, pp. 543-574.

[10] J.J. Monaghan, *Simulating free surface flows with SPH,* Journal of Computational physics, 110 (1994),pp. 399-406.

[11] J.J. Monaghan, *Smoothed particle hydrodynamics,* Reports on Progress in Physics 68, 8 (2005),pp. 1703-1759.

[12] G.R. Liu, M.B. Liu, *Smooth Particle Hydrodynamics a Meshfree Particle Method,* World Scientific Publishing, London, 2003.

[13] M. Becker, M. Teschner, *Weakly compressible SPH for free surface flows,* Eurographics/ ACM SIGGRAPH Symposium on Computer Animation , 2007, pp. 1-8.

[14] T. Yamazaki, S. Omata, K. Švadlenka, K. Ohara, *Construction of approximate solution to a hyperbolic free boundary problem with volume constraint and its numerical compution,* Advances in Mathematical Sciences and Applications, 16 (2006),pp. 57-67.

[15] K. Švadlenka, *Mathematical analysis and numerical computation of volume-constrained evolutionary problems, involving free boundaries,* PhD. thesis, Kanazawa University, Japan, 2008.

[16] K. Švadlenka, *A new numerical model for propagation of tsunami waves,* to appear in Kybernetika 43 (6), 2007.

[17] E. Ginder, K. Švadlenka, *A variational approach to a constrained hyperbolic free boundary problem,* Nonlinear Analysis 71, 2009, pp. e1527-e1537.

[18] M. Kazama, S. Omata, *Modelling and computation of fluid-membrane interaction,* Nonlinear Analysis 71 (2009), pp. e1553-e1559.

[19] T. Young, *An essay on the cohesion of fluids,* Philos. Trans. R. Soc. London, 95(1805),pp. 65-87.

[20] K. Švadlenka, S. Omata, *Mathematical modelling of surface vibration with volume constraint and its analysis,* Nonlinear Analysis 69, 2008, pp. 3202-3212